Extracellular adenosine deamination primes tip organizer development in *Dictyostelium*

Pavani Hathi and Ramamurthy Baskar*

Bhupat and Jyoti Mehta School of Biosciences, Department of Biotechnology, Indian Institute of Technology-Madras, Chennai 600036, India.

*Correspondence: rbaskar@iitm.ac.in

Abstract

Ammonia is a morphogen in *Dictyostelium* and is known to arise from the catabolism of proteins and RNA. However, we show that extracellular adenosine deamination catalyzed by 'adenosine deaminase related growth factor' (ADGF), is a major source of ammonia, and demonstrate a direct role of ammonia in tip organizer development. The tip formed during early development in *Dictyostelium* functions analogously to the embryonic organizer of higher vertebrates. *Dictyostelium* cell lines carrying mutations in the gene *adgf* fail to establish an organizer, and this could be reversed by exposing the mutants to volatile ammonia. Interestingly, *Klebsiella pneumoniae* physically separated from the *Dictyostelium adgf* mutants in a partitioned dish, also rescues the mound arrest phenotype suggesting a cross-kingdom interaction that drives development. Both the substrate, adenosine and the product, ammonia regulate *adgf* expression, and ADGF acts downstream of the histidine kinase DhkD in regulating tip formation. Thus, the consecutive transformation of extracellular cAMP to adenosine, and adenosine to ammonia are integral steps during *Dictyostelium* development. Remarkably, in higher vertebrates, *adgf* expression is elevated during gastrulation and thus adenosine deamination may be a conserved process driving organizer development in different organisms.

23 **Key words**

24 adenosine deaminase, organizer development, tip formation, volatile ammonia, *Dictyostelium*

25 Introduction

26 During early embryonic development, organizers play an important role in patterning and
27 directing the differentiation of surrounding cells into specific tissues and organs. The embryonic
28 organizer establishes the developmental polarity in vertebrates; and similarly, in *Dictyostelium,*
29 the mound/slug tip acts as an organizer (Rubin and Robertson, 1975) playing a pivotal role in
30 guiding collective cell migration and patterning. Despite numerous investigations on
31 *Dictyostelium* tip formation, the processes by which the tip establishes and maintains the primary
32 developmental axis remains elusive. Gaining insights into the mechanisms regulating tip
33 organizer function will offer valuable insights on orchestrated cell movements and processes
34 underlying development.

35 *Dictyostelium* transitions from a unicellular amoeba to a multicellular organism in response to
36 starvation. The cells aggregate into a mound, which gives rise to a migrating slug and ultimately
37 a fruiting body composed of spores and a dead stalk (Raper, 1940; Kessin, 2001). This process is
38 regulated by diffusible signals including cAMP, adenosine, ammonia, and a chlorinated
39 hexaphenone, 'differentiation-inducing factor' (DIF) (Bloom and Kay, 1988; Williams, 1988;
40 Gross, 1994; Mahadeo and Parent, 2006). Importantly, the cell cycle phase soon after starvation
41 is known to strongly influence the cell fate either as prestalk (pst) or prespore (psp) cells (Weeks
42 and Weijer, 1994; Jang and Gomer, 2011).

43 Tip development in *Dictyostelium* depends on cAMP signaling in turn regulating protein kinase
44 A (PKA) activity, adenosine signaling, and morphogenetic cell movements (Schaap and Wang,

45 1986; Mann and Firtel, 1993; Siegert and Weijer, 1995). Adenosine, a by-product of cAMP
46 hydrolysis, acts as an inhibitory morphogen suppressing additional tip formation (Schaap and
47 Wang, 1986).

48 Adenosine deaminases (ADA) catalyse the breakdown of adenosine to generate inosine and
49 ammonia, and are conserved among bacteria, invertebrates, vertebrates including mammals
50 (Cristalli et al., 2001). In humans, two isoforms of ADA are known including ADA1 and ADA2,
51 and the *Dictyostelium* homolog of ADA2 is adenosine deaminase-related growth factor (ADGF).
52 Unlike ADA that is intracellular, ADGF is extracellular and also has a growth factor activity (Li
53 and Aksoy, 2000; Iijima et al., 2008). Loss-of-function mutations in *ada2* are linked to
54 lymphopenia, severe combined immunodeficiency (SCID) (Gaspar, 2010), and vascular
55 inflammation due to accumulation of toxic metabolites like dATP (Zhou et al., 2014;
56 Notarangelo, 2016). In mice, *ada2* disruption leads to perinatal mortality (Wakamiya et al.,
57 1995), and overexpression of *ada2* results in aberrant heart and kidney development (Riazi et al.,
58 2005). In frogs, mutations in *ada2* manifest in reduced body size and altered polarity (Iijima et
59 al., 2008). In *Drosophila*, certain isoforms of ADGF are known to play a pivotal role in cell
60 proliferation by depleting extracellular adenosine (Zurovec et al., 2002), and loss of function of
61 *adgfA* promotes melanotic tumour formation and larval death (Dolezal et al., 2005). Adenosine
62 deaminases are known to interact with dipeptidyl peptidase IV (DPP), cluster of differentiation
63 (CD26) expressed on T-cells and the adenosine receptor, A2AR (expressed on dendritic cells) to
64 facilitate cell-cell signaling (Moreno et al., 2018). Thus, *adgf* plays a pivotal role in the
65 regulation of cell proliferation and development in several organisms.

66 Four isoforms of ADA are annotated in the *Dictyostelium discoideum* genome (Eichinger et al.,
67 2005) including adenosine deaminase (*ada*; DDB_G0287371), adenosine deaminase acting on

68 tRNA-1 (DDB_G0278943), adenosine deaminase tRNA-specific (DDB_G0288099) and
69 adenosine deaminase-related growth factor (*adgf*; DDB_G0275179), and their role in growth and
70 development is not known. In this study, we demonstrate that ammonia generated by ADGF
71 plays a direct role in establishing the tip organizer, highlighting a novel link between nucleoside
72 metabolism and developmental polarity in *Dictyostelium*.

73 **Results**

74 **Differential regulation of *adgf* expression during growth and development**

75 *Dictyostelium* cell lines carrying mutations in the gene *adgf* were obtained from the genome wide
76 *Dictyostelium* insertion (GWDI) bank, and were subjected to further analysis to know the role of
77 *adgf* during *Dictyostelium* development. To verify the insertion of blasticidin *(bsr)* resistance
78 cassette in *adgf* mutant, a diagnostic PCR was carried out and the integration was validated
79 (Figures 1A and 1B), and qRT-PCR analysis confirmed the absence of *adgf* expression (Figure
80 1C). In vertebrates, adenosine deaminases are expressed in a tissue specific manner to control
81 growth and development. To determine whether *adgf* expression is differentially regulated
82 during *Dictyostelium* development, qRT-PCR was performed using RNA isolated at 0 h, 8 h, 12
83 h, 16 h, 20 h and 24 h post starvation. *adgf* expression peaks at 16 h (Figure 1D) implying an
84 important role for *adgf* later in development. At this time point, the expression of the other three
85 isoforms of ADA were not significantly different from wild-type (WT), suggesting that the loss
86 of *adgf* (data not shown) function is not compensated by the other isoforms.

87 **The predicted structures of *Dictyostelium* ADGF and human ADA2 share a strong**
88 **structural similarity.**

89 The *D. discoideum adgf* gene is predicted to encode a protein of 543 amino acids, and belongs to
90 the metallo-transferases superfamily (Figure S1A), having an ADA and an N- terminal domain
91 similar to human ADA2 (Figure S1B). The ADGF sequence from the protein family database
92 (https://www.ebi.ac.uk/interpro/) was analysed using the online tool SMART (Simple Modular
93 Architecture Research Tool: http://smart.embl-heidelberg.de), to know the presence of
94 structurally similar domains. The different domains of *Dictyostelium* ADGF (DdADGF) show a
95 high degree of similarity with human ADA2. DdADGF shares 37.5% identity with human
96 ADA2 and shares a sequence similarity of 59.5% with *D. fasciculatum*, 61.2% with *D. pupureum,*
97 53.6% with *D. lacteum* and 62.1% with *Polysphondylium pallidum* (www.uniprot.org). Multiple
98 sequence alignment reveals the presence of an N-terminal signal sequence characteristic of
99 extracellular proteins (Figure S1C).and conserved histidine and glutamine residues in the active
100 site of both *D. discoideum* ADGF and human ADA2 (Figure S1D).

101 The phylogenetic relation of ADGF to the classic ADA subfamily has been reported previously
102 (Maier et al., 2005). To determine the evolutionary relationship of DdADGF with that of other
103 organisms, a phylogenetic analysis was carried out, and the amino acid alignment was created
104 using MEGAX software (Kumar et al., 2018). The evolutionary history of ADGF was inferred
105 using a Maximum Likelihood approach with Bootstrap analysis (100 iterations) as described by
106 Felsenstein (1985). The resulting phylogenetic tree indicated that DdADGF is closely related to
107 the ADGF proteins of other Dictyostelids, including *D. purpureum*, *Heterostelium pallidum,* and
108 *Cavenderia fasciculata*. DdADGF forms a distinct clade, likely representing a distant relative of
109 its vertebrate homolog (Figure S1E). Using the crystal structure of human ADA2, Cat eye
110 syndrome critical region protein 1 (CECR1) as a template (PDB-3LGD), the structure of
111 DdADGF was predicted by homology modeling (https://alphafold.ebi.ac.uk/) (Figures S1 F-H).

112 Alignment of DdADGF with human ADA2 yielded a root mean square deviation (RMSD) value
113 of 1 Å, indicating strong structural similarity (Eidhammer et al., 2000; Koehl, 2001).

114 ***adgf* controls aggregate size in *Dictyostelium***

115 To understand the role of *adgf* during *D. discoideum* development, *adgf* mutants were plated at a
116 density of $5x10^5$ cells/cm^2 on non-nutrient phosphate buffered agar plates and monitored
117 thereafter. In comparison to WT, the aggregates of *adgf* $^-$ were larger, and thus the number of
118 aggregates were fewer (Figure 2A) than the WT. To determine the pathways impairing the tissue
119 size in the mutant, RNA expression of countin (*ctn*) and small aggregates (*smlA*) were examined,
120 and their levels were reduced significantly compared to controls (Figure 2B). Countin factor (CF)
121 regulates group size by reducing the expression of cell-cell adhesion proteins cadherin (*cadA*)
122 and contact site A (*csaA*) (Siu et al., 1985; Coates and Harwood, 2001). Compared to WT, both
123 cell-to-cell adhesion and *cadA, csaA* expression were higher in the *adgf* mutant (Figures 2C and
124 2D) suggesting that *adgf* regulates the overall size of the aggregates.

125 cAMP chemotaxis significantly influences cell-cell adhesion (Konijn et al., 1967), and to
126 determine if chemotaxis is impaired in the *adgf* $^-$ lines, an under-agarose chemotaxis assay was
127 carried out. The chemotactic activity was not significantly different between the two cell types
128 (Figure 2E), suggesting that the increased mound size in the mutant is not due to altered
129 chemotaxis.

130 ***adgf* mutants form large, tipless mounds**

131 Subsequent to plating on KK2 agar, WT cells formed mounds by 8-9 h, and culminate to form
132 fruiting bodies by the end of 24 h. In contrast, the *adgf* $^-$ lines were blocked as rotating mounds
133 with no tips till 30 h (Figure 2F; Supplementary videos S1 and S2). Such a mound arrest

134 phenotype could be mimicked by adding the ADA specific inhibitor deoxycoformycin (DCF) to
135 WT cells (Figure 2G). After 36 h, a fraction of *adgf* $^{-}$ mounds (34.77 ± 4%) formed fruiting
136 bodies with bulkier spore sac (79.6 ± 6.3 mm^2) and stalk (Figures 2H and 2I). This late recovery
137 from the mound arrest may be due to the expression of other ADA isoforms after 36 h.

138 **Reduced ADA activity leads to high adenosine levels in the *adgf* mutant**

139 If *adgf* function is compromised, ADA enzyme activity is expected to be low. To verify this,
140 total ADA activity in WT and *adgf* $^{-}$ mounds was measured using a commercial assay kit. This
141 assay relies on the conversion of inosine (derived from ADA activity) to uric acid, and was
142 measured spectrophotometrically. Although ADA activity dropped significantly in the mutant
143 (Figure 3A), it was not completely abolished, and possibly, other isoforms may have a basal
144 activity both at 12 h and 16 h.

145 ADGF quenches extracellular adenosine, and if blocked, as expected in *adgf* $^{-}$*,* the mutants will
146 have increased extracellular adenosine. Using a commercial kit, the total adenosine levels were
147 measured, and both at 12 h and 16 h, the levels were elevated (Figure 3B), and this difference
148 was highly significant at 16 h. *adgf* expression at this time point was also high in WT cells. The
149 elevated adenosine levels at 16 h may result from reduced ADA activity and increased
150 expression of genes such as 5' nucleotidase (*5'nt*) and phosphodiesterases (*pdsA* and *regA*)*,* all
151 involved in adenosine formation (Headrick and Willis, 1989; Godecke, 2008). Hence, their
152 expression levels were examined. Although the expression of both *5'nt* and *regA* were enhanced
153 at 8 h, *pdsA* levels remained unaltered. Interestingly, the expression of all three genes trended
154 lower at 12 h but were significantly upregulated at 16 h (Figure 3C), suggesting an important
155 role of these genes at a specific time in development.

156 **Addition of ADA or overexpression of *adgf* cDNA restored tip development in *adgf*$^{-}$**

157 *adgf* mutants carry significantly high levels of adenosine. By administering ADA enzyme on top
158 of the *adgf*$^{-}$ mounds (Figure 4A), excess adenosine can be quenched resulting in ammonia
159 formation, possibly rescuing the phenotype. Indeed, addition of 10 U ADA onto mutant mounds
160 restored tip development. Besides, overexpression of WT *adgf* cDNA (driven by actin15
161 promoter) complemented the developmental defects of *adgf* mutants (Figures 4B and 4C),
162 confirming that the developmental block is the result of *adgf* gene disruption alone. However,
163 *adgf* cDNA overexpression in WT cells does not result in any observable defects (Figure 4D).
164 Taken together, these findings support an important function of *adgf* in tip development.

165 **WT or its conditioned media (CM) restored tip formation in *adgf*$^{-}$ mounds**

166 To determine whether *adgf* is necessary for tip formation in a cell-autonomous manner, WT and
167 the mutant cells were mixed in different proportions and plated for development. In a mix of
168 50% WT: 50% mutant, the mound defects of *adgf*$^{-}$ were rescued, but with 20% WT and 80%
169 *adgf*$^{-}$, the rescue was partial (31 ± 4 %) (Figure 4E) suggesting that the mound arrest phenotype
170 of the mutant is due to the absence of some secreted factor(s).

171 Further, when developed in the presence of WT CM, *adgf*$^{-}$ cells formed tipped mounds and
172 eventually fruiting bodies (Figure 4F). Conversely, in the presence of *adgf*$^{-}$ CM, WT cells
173 developed as large mounds with no tips (Figure 4G) and the size was comparable to the mounds
174 formed by *adgf*$^{-}$. These findings imply that the developmental phenotype of *adgf*$^{-}$ is not due to a
175 cell autonomous defect but due to faulty secreted factor signaling. While this finding is
176 consistent with the involvement of a secreted factor, it is also possible that a membrane-bound
177 extracellular factor may have a role in complementing the mutant phenotype.

178 **Volatile ammonia rescued the mound arrest phenotype of *adgf*⁻**

179 If ADGF enzyme activity is compromised, ammonia levels are expected to be low. Hence, the
180 concentration of ammonia from WT and *adgf*⁻ mounds was measured using a commercial kit.
181 Ammonia levels were significantly reduced in *adgf*⁻ lines (Figure 5A). By mixing sodium
182 hydroxide and ammonium chloride (Thadani et al., 1977), ammonia could be generated, and in
183 such conditions, tip formation was restored in *adgf*⁻ mounds (Figure 5B). All the rescue
184 experiments involving ammonia were carried for a 3.5 h time period.

185 **Physically separated WT restored tip development in the mutant**

186 WT mounds are expected to release different set of volatiles including ammonia, possibly
187 rescuing the mound arrest phenotype of the mutants nearby. To verify if this is correct, *adgf*⁻
188 cells were developed in one half of a compartmentalized Petri dish, and WT cells on the other
189 side. Interestingly, the mound arrest of *adgf*⁻ was fully rescued (Figure 5C) in the presence of
190 WT, although they were physically separated from each other. This suggests that volatiles, likely
191 to be ammonia released from WT is sufficient enough to rescue the mutant phenotype.

192 The *adgf*⁻ CM is expected to have high adenosine levels, possibly generating low or no
193 ammonia. Addition of ADA to *adgf*⁻ CM in one compartment of the partitioned dish led to
194 partial rescue (57 % ± 2) of *adgf*⁻ kept on the other side of the dish (data not shown) implying
195 that the ammonia generated in such conditions may not be enough for a full rescue.

196 **Adenosine deamination alone drives the rescue of *adgf*⁻**

197 To know if adenosine deamination is exclusively responsible for the rescue of the mutant, 10 ml
198 cold KK2 buffer mixed with different concentrations of adenosine (10 μM, 0.1 mM, 1 mM) was
199 added in one half of the compartmentalized dish, and the other side of the dish had the mutant on

200 phosphate buffered agar arrested at the mound stage. Addition of ADA enzyme (10 U) to the
201 buffered solution containing adenosine led to a full rescue after 3.5 h (Figure 5D), strongly
202 indicating that volatile ammonia generated from adenosine deamination alone is rescuing the
203 defect. Protein/RNA catabolism also generates ammonia in *Dictyostelium* (White and Sussman,
204 1961; Hames and Ashworth, 1974; Schindler and Sussman, 1977; Walsh and Wright, 1978), but
205 their levels were not significantly different between WT and *adgf* mutants (Figure S2A-B)
206 suggesting that ammonia released from adenosine deamination plays a direct role in tip
207 formation.

208 **Caffeine, not ammonia rescued the mound size of *adgf*$^{-}$**

209 Given that adenosine levels were elevated in the mutants, we attempted to rescue the large
210 mound size observed in the *adgf* mutants by treating them with the adenosine receptor antagonist,
211 caffeine (Costenla et al., 2010; Ribeiro and Sebastiao, 2010). Caffeine rescued this early
212 developmental defect in a dose-dependent manner (Figure 5E), suggesting that *adgf* may be one
213 of the regulators of group size in *Dictyostelium*. Since ammonia levels were reduced in the
214 mutant, we tested whether exposure to ammonia could rescue the large mound size of the *adgf*
215 mutant. Exposing the mutants to 0.01 M ammonia soon after plating or six hours after plating,
216 had no effect on the mound size of the mutants (Figure 5F), suggesting that while some early
217 effects may be mediated through adenosine receptors, the later effects appear to be independent
218 and are likely to be influenced by ammonia.

219 **Faulty expression of cAMP relay genes in *adgf*$^{-}$**

220 cAMP signaling is crucial for tip development and determining cell fate in *Dictyostelium*
221 (Schaap and Wang, 1986; Saxe et al., 1993; Firtel, 1996; Singer et al., 2019). Hence, the
222 expression of genes involved in cAMP relay were measured in WT and *adgf*$^{-}$ cells by qRT-PCR.

223 Total cAMP levels and *acaA* gene expression were both low in the *adgf*$^-$ lines (Figures 6A and
224 6B). Treating the cells with the pkA activator 8-Br-cAMP or the activator of adenyl cyclase,
225 cyclic-di-GMP (Wang and Schaap, 1985; Chen and Schaap, 2012), reversed the *adgf*$^-$ mound
226 arrest phenotype (Figures 6C and D), and increasing the cyclic-di-GMP dose from 0.5 mM to 1
227 mM resulted in multi tipped phenotype (Figure 6E). These observations reinforce that the mound
228 arrest phenotype of the *adgf*$^-$ lines is due to faulty cAMP signaling. A transient increase in
229 cAMP levels can be achieved by blocking the phosphodiesterase (*pde4*) activity. When treated
230 with a known PDE4 inhibitor, 3-Isobutyl-1-methylxanthine (IBMX) (Bader et al., 2007; Siegert
231 and Weijer, 1989), there was no effect on tip formation in *adgf*$^-$ mounds (Figure 6F), although
232 caffeine restored tip formation (Figure 6G).

233 **Circular instead of spiral cAMP waves in *adgf*$^-$ mounds**

234 Low *acaA* expression, reduced cAMP levels and enhanced cell-cell contacts in *adgf*$^-$ is likely to
235 impair cAMP wave propagation, and to ascertain if this is true, the cAMP signal propagation in
236 WT and *adgf*$^-$ mounds were compared using dark field optics. The cAMP wave propagation was
237 spiral in WT, and in contrast, the waves were circular in the *adgf* mutant, suggesting that the
238 cAMP relay is impaired (Figure 6H; Supplementary videos S3 and S4). While this strongly
239 suggests a defect in the mutant's ability to sustain spiral wave formation, the possibility of short-
240 lived or transient spiral waves in the mutant cannot be excluded.

241 **Ammonia restores tip formation by regulating *acaA/pde4* expression**

242 To find if *adgf* expression is regulated by the substrate or the product, WT cells were treated with
243 different concentrations of adenosine (100 nM, 1 µM, 0.5 mM), plated on KK2 agar plates and
244 harvested at 16 h for RNA isolation. Independently, WT mounds on KK2 agar plates were
245 exposed to different concentrations of volatile ammonia (0.1 mM, 1 mM, 10 mM) for 3 h and

246 thereafter, the mRNA expression levels of *adgf*, *acaA* and *pde4* were examined. With 100 nM
247 adenosine, the expression of both *adgf* and *acaA* decreased, but at higher adenosine
248 concentrations (1 μM, 0.5 mM), the expression levels of these two genes were comparable to
249 controls (Figure 7A). Interestingly, *pde4* expression decreased gradually with increasing
250 adenosine concentrations (100 nM to 0.5 mM), but increased steadily with increasing ammonia
251 levels.

252 Exposure of WT mounds to 0.1 mM ammonia, led to decreased *adgf* expression but exposure to
253 1 mM and 10 mM ammonia, respectively caused a 3 and 2.3-fold upregulation of *acaA*
254 expression. These observations suggest that ammonia may be rescuing the mound arrest
255 phenotype by enhancing *acaA* expression and thus cAMP levels. In similar conditions, a
256 considerable increase in *pde4* expression was observed (Figure 7B), which may be necessary for
257 controlling cAMP levels in response to ammonia treatment. In conclusion, the expression of *adgf*
258 is influenced both by the substrate adenosine, as well as the product ammonia in a dose
259 dependent manner. To ascertain if ammonia exposure indeed increases the cAMP levels in the
260 mutant thereby restoring the phenotype, cAMP levels were measured in the *adgf* mutant mounds
261 following the rescue with ammonia. Indeed, the cAMP levels were higher in the rescued mounds
262 compared to untreated *adgf* controls (Figure 7C), supporting the idea that ammonia promotes tip
263 development by restoring the cAMP signaling.

264 ***adgf*$^{-}$ cells sort to prestalk in a chimera with WT**

265 To determine if *adgf* favours the differentiation of one cell type over the other, the expression of
266 pst and psp markers were examined in the mutant by realtime PCR. While the expression of pst
267 markers, *ecmA* and *ecmB* were significantly upregulated, the psp-specific *pspA* gene expression
268 was reduced in the mutant (Figure 7D), suggesting that WT *adgf* favours psp expression.

269 To know the cell type preference of the *adgf* mutants in a chimera with WT, a fraction (20%) of
270 any one cell type was labelled with a cell tracker stain 1,1'-Dioctadecyl-3,3,3',3'-
271 Tetramethylindocarbocyanine Perchlorate (DIL), and the development was tracked thereafter. In
272 the slugs that formed after mixing labelled WT or *adgf* ^{OE} cells with 80% unlabelled *adgf* $^{-}$ cells,
273 the fluorescence was largely confined to the psp region (Figures 8B-C). Conversely, when *adgf* $^{-}$
274 cells stained with DIL were mixed with unlabelled WT or *adgf* ^{OE}, the fluorescence was
275 restricted to the pst part of the slug (Figure 8A). In the chimeric slugs, consistently, labelled WT
276 or *adgf* ^{OE} cells occupy the psp, whereas the *adgf* $^{-}$ cells end up in the pst region. Thus, the
277 distribution of cell types in the mound/slug is significantly influenced by *adgf,* as the mutant
278 cells sort out in a mixture with WT cells and differentiate to pst cells.

279 Further, when *adgf* $^{-}$ slugs were stained with the pst marker, neutral red (Yamamoto and
280 Takeuchi, 1983), the staining was intense in the pst region and anterior-like cells (ALCs), and
281 such an intense coloration was not apparent in WT especially in the ALCs (Figure S3A). To
282 further investigate if reduced ADA activity affects cell type specific marker expression or their
283 pattern in slugs, pst (*ecmA*-GFP, *ecmO*-GFP) or psp (*pspA*-RFP) lines were treated with the
284 ADA inhibitor DCF. While there was no change in pst/psp patterns in the fraction of mounds and
285 slugs that developed after a long delay, the *ecmA*-GFP fluorescence was intense when compared
286 to WT (Figures S3B). Similar to NR staining pattern in *adgf* mutant slugs, a prominent
287 expression of *ecmA*-GFP was observed in the ALC region also. Visually, there was no change in
288 *ecmO* or *pspA* marker expression in DCF treated slugs (Figures S3C and S3D) suggesting that
289 impaired ADGF activity affects tip specific expression.

290 To know if *adgf* expression is differentially regulated between the two major cell types, psp-GFP
291 tagged WT slugs were disaggregated, and using the fluorescence activated cell sorter (FACS),

292 GFP-negative prestalk (pst-GFP^{-}) and GFP-positive prespore (psp-GFP^{+}) populations were
293 obtained (Figures 9A-E), and RNA was isolated from both cell populations. Real time PCR
294 analysis reveals that *adgf* expression is 4.95-fold higher in the psp-GFP^{+} than pst-GFP^{-} cells
295 (Figure 9F). The preferential sorting of WT cells to psp region and the *adgf* mutants (with
296 reduced psp expression) to the pst part of the slug also reinforces the differential expression of
297 *adgf*. Thus, cells with higher *adgf* expression preferentially sorted to the psp region and the
298 absence of *adgf* in mutant cells may hinder their ability to adopt a prespore fate, leading to their
299 preferential sorting in the pst region within the chimera.

300 ***adgf* acts downstream of the histidine kinase, *dhkD***

301 In an effort to identify the pathway by which *adgf* acts during tip development, we selected a
302 number of mutant lines with similar mound arrest phenotype such as cAMP receptor B (*carB* $^{-}$),
303 LIM domain containing protein (*limB* $^{-}$), mound mutant (*mndA* $^{-}$) and histidine kinase (*dhkD* $^{-}$)
304 (Saxe et al., 1993; Carrin et al., 1996; Chien et al. 2000; Singleton and Xiong, 2013), and treated
305 the mounds with ADA enzyme. Treatment with 10 U ADA or exposure to ammonia restored tip
306 formation in *dhkD* $^{-}$ mounds and not others tested (Figures S4A and S4C). An increase in ADA
307 concentration (20 U), resulted in the development of multiple tips in *dhkD*$^{-}$ (Figures 10A-C).
308 Further, in the *dhkD* mutant mounds that were rescued by ammonia, cAMP levels were
309 significantly elevated compared to untreated *dhkD* $^{-}$ controls (Figure S4D). These findings imply
310 that ammonia induced tip formation increased cAMP levels, thereby restoring the phenotype, and
311 *adgf* acts downstream of *dhkD* in controlling tip development. Similarly, we tested few mutants
312 with multi-tipped phenotype, such as tipped mutant (*tipA* $^{-}$), culinB (*culB* $^{-}$), autophagy mutants
313 (*atg7* $^{-}$, *atg8*$^{-}$, and *atg9*$^{-}$) (Stege et al., 1999; Wang and Kuspa, 2002; Otto et al., 2003; Otto et al.,
314 2004, Tung et al., 2010) by adding the ADA inhibitor, DCF (1 mM) to the cell suspension /agar

315 plates and if rescued, those mutants are likely to be in the same pathway as that of *adgf* in
316 controlling tip development. However, DCF treatment had no impact on the phenotype of the
317 mutants with multiple tips (Figure S4B).

318 **Impaired expression of other deaminases also results in aberrant tip formation**

319 Several pathways control ammonia levels during development, and knockouts in other
320 deaminases (2-aminomuconate deaminase: DDB_G0275081, adenosine monophosphate
321 deaminase: DDB_G0292266, dCTP deaminase: DDB_G0293580, threonine deaminase:
322 DDB_G0277245, N-acetyl glucosamine deaminase: DDB_G0286195, glucosamine-6-phosphate
323 deaminase: DDB_G0278873) show a partial mound arrest phenotype (Figures S5A-F) although
324 the expression of some of these candidates is stronger during development, suggesting a
325 prominent and unique role of adenosine deamination in tip development.

326 **High adenosine levels and other related purines do not block tip development**

327 ADA catalyses the conversion of adenosine/deoxy adenosine respectively to inosine/ deoxy
328 inosine. As *adgf* mutants have high adenosine levels, we investigated if the mound arrest could
329 be mimicked in WT by treating with adenosine. However, addition of adenosine does not lead to
330 mound arrest in WT (Figure S6A). It is possible that ADA/ADGF converted adenosine
331 analogues to inosine analogues, which in some manner affected development. Hence, WT cells
332 were treated with adenosine analogue (2'-deoxyadenosine) or guanosine (10 μM each), and they
333 do not cause a mound arrest phenotype either. Similarly, treating *adgf*$^{-}$ mounds with inosine
334 does not restore tip formation (Figures S6B and S6C) suggesting that the blocked tip
335 development is due to faulty adenosine deamination alone.

336 **Cross kingdom rescue of the *adgf*$^{-}$ mound arrest phenotype**

337 Just like WT *Dictyostelium* rescuing the mound arrest phenotype of the *adgf* mutant, we
338 examined if bacteria physically separated from the mutants would rescue the phenotype. To
339 check this, *Klebsiella pneumoniae* and *adgf* mutants were incubated adjacent to each other within
340 a compartmentalized KK2 agar plate. After 12 h incubation period, tip formation was restored in
341 the mutants while in the same time frame, the mounds in controls failed to form tips. Possibly,
342 *Klebsiella* on KK2 plates with no nutrients would die releasing ammonia thereby restoring tip
343 development in *Dictyostelium* (Figure S7).

344 **Discussion**

345 ***Dictyostelium* ADGF is likely to be a secreted growth factor**

346 Multiple sequence alignments, experiments with conditioned media and cell mixing with WT
347 suggests that ADGF is secreted. ADGF is also known to interact with 5′-adenosine
348 monophosphate (AMP) and deoxyadenosine. AMP deaminase, previously characterized in the
349 mollusk *Helix pomatia*, has been identified as a member of ADGF family (Tzertzinis et al.,
350 2023). Studies on the characterization and expression of ADGF in Pacific abalone has shown
351 that it is a secreted protein critical for embryonic and larval development (Hanif et al., 2022).
352 The crystal structure of human ADA2 reveals the presence of a catalytic- and two unique ADA2-
353 specific domains with novel folds, responsible for protein dimerization and interaction with cell
354 surface receptors. Furthermore, the presence of a number of N-glycosylation sites, conserved
355 disulfide bond, and a signal peptide indicate that ADA2 is specifically adapted to function in the
356 extracellular environment (Zavialov et al., 2010).

357 **Possible reasons for increased mound size in the *adgf* mutant**

358 Enhanced cell adhesion influences cohesion and can impact the mound size (Roisin-Bouffay et
359 al., 2000). The expression of *cadA* and *csaA* genes were upregulated in the *adgf* mutant, possibly
360 leading to increased adhesion and larger mound formation. While over-secretion of *ctn* leads to
361 stream breaking and small aggregate formation (Brock and Gomer, 1999), disruption of the *ctn*
362 gene prevents this process, inducing large aggregate formation. *ctn* in turn regulates *smlA* (Brock
363 et al., 2003), impacting the overall aggregate size. Thus, *adgf* mutants that have reduced *ctn* and
364 *smlA* expression manifest in large mound formation. Indeed, cells treated with adenosine are
365 known to form large aggregates (Schaap and Wang, 1986; Jaiswal et al., 2012), and the first
366 genetic evidence supporting the previous work is from *adgf* mutants, which carry excess
367 extracellular adenosine and form large aggregation streams.

368 **Pathways generating ammonia in *Dictyostelium***

369 Ammonia can come from a variety of sources both within and outside the cells and this can be
370 from dead cells also. Proteolysis during starvation is believed to be the main source of volatile
371 ammonia in *Dictyostelium* (Hames and Ashworth, 1974; Schindler and Sussman, 1977; White
372 and Sussman, 1961), while RNA degradation is also attributed to yield ammonia during
373 starvation (Walsh and Wright, 1978). During development, amino acids, total protein and RNA
374 levels are reported to reduce with a significant increase in ammonia levels, thus equivocating the
375 source of volatile ammonia (Hames and Ashworth, 1974). The highly acidic, autophagic vesicles
376 in pst cells (Gross, 2009) are believed to catalyze the breakdown of proteins and RNA, also
377 generating ammonia.

378 Furthermore, several deaminases or enzymatic reactions in *Dictyostelium* may also generate
379 ammonia (Supplementary Table S1). The annotated *D. discoideum* genome contains five
380 evolutionarily conserved family of ammonium transporter/methylammonium permease/rhesus

381 protein (Amt/Mep/Rh) encoding genes (Eichinger et al., 2005), *amtA, amtB, amtC, rhgA,* and
382 *rhgB,* which help in regulating ammonia levels during growth and development. *amtA* and *amtC*
383 antagonistically control developmental processes and are involved in ammonium sensing or
384 transport (Follstaedt et al., 2003; Kirsten et al., 2005; Singleton et al., 2006).

385 **Role of ammonia during *Dictyostelium* development**

386 Ammonia is known to inhibit aggregation (Schindler and Sussman, 1979; Williams et al., 1984),
387 affect aggregate territory size (Thadani et al., 1977), aggregate density (Feit, 1988), cell fate
388 (Gross et al., 1988), culmination (Davies et al., 1993) and fruiting body size in *Dictyostelium*
389 (Lonski, 1976). Ammonia promotes psp over pst differentiation (Newell et al., 1969; Sternfeld
390 and David, 1979; Gross et al. 1983; Oyama and Blumberg, 1986), and favors prolonged slug
391 migration called 'slugging' over culmination by suppressing DIF biosynthesis (Neave et al.,
392 1983). Ammonia plays a crucial role in orienting cell masses, accelerating the movement of
393 aggregating cells (Bonner et al., 1986), and prevents the developmental transition of slugs to
394 fruiting bodies (Bradbury and Gross, 1989; Wang and Schaap, 1989). Enzymatic removal of
395 ammonia causes the quick transition from slug to fruiting thus controlling the morphogenetic
396 pathways (Schindler and Sussman, 1977).

397 Beyond its broad effects on aggregation and culmination, ammonia also reinforces positional
398 information by elevating intracellular cAMP levels, favoring prespore over prestalk
399 differentiation (Bradbury and Gross, 1989; Riley and Barclay, 1990; Hopper et al., 1993).
400 Ammonia is known to influence rapid patterning of *Dictyostelium* cells confined in a restricted
401 environment (Sawai et al., 2002). In *adgf* mutants that have low ammonia levels, both neutral red
402 staining and the prestalk marker *ecmA/ ecmB* expression are higher than the WT, and the mound
403 arrest phenotype can be reversed by exposing the *adgf* mutant mounds to ammonia. As a gas,

404 ammonia can diffuse generating a gradient. The slime sheath at the back of the slug is believed to
405 prevent the diffusion of ammonia (Gross, 2009), and ammonia escaping through the slug front
406 neutralizes the acidic vesicles in prestalk cells (Bonner, 1952). Thus, a rise in the pH of these
407 acidic vesicles and the cytoplasm (Poole and Ohkuma, 1981; Gross et al, 1983; Davies et al
408 1993), is known to increase the speed of chemotaxing amoebae (Siegert and Weijer, 1989; Van
409 Duijn and Inouye, 1991), favouring collective cell movement (Bonner et al., 1988, 1989), and
410 tipped mound development. Thus ammonia actively promotes the transition from mound to
411 tipped mound formation.

412 Our results (Figure 6A) also show that the amount of ammonia released from adenosine is in the
413 same order of magnitude as that from other sources (Yoshino et al., 2007). It is interesting that a
414 mutation in *adgf* manifests in arrested tip development, although *adgf* expression was found to
415 be higher in psp than pst cells. If a threshold concentration of ammonia is not present, collective
416 cell movement influencing tip formation may be blocked at the mound stage. Increased *adgf*
417 expression in psp than pst cell types suggest that low extracellular adenosine (Weijer and
418 Durston, 1985; Schaap and Wang, 1986) and high levels of ammonia influence psp cell fate. The
419 decision between the formation of the tip (pst cells) and the ALC is controlled by the tip's
420 production of ammonia, which prevents the migration of ALCs towards the tip (Sternfeld and
421 David, 1982; Feit et al., 1990).

422 In slugger mutants, ammonia is known to inhibit tip formation (Gee et al., 1994), but not in WT
423 NC4. Yoshino et al., (2007) have also reported ammonia inhibiting both aggregation and tip
424 formation in WT cells. However, ammonium chloride was used as a source of ammonia, and the
425 potential interference from chloride ions cannot be ruled out. A mutant impaired in

426 mitochondrial function, *midA*⁻, is reported to accumulate high levels of ammonia that inhibited
427 development (Torija et al., 2006). Notably, these cells were developed with overhead light, a
428 condition that may influence ammonia sensitivity and the developmental phenotype. However,
429 ammonia exerts no effect on tip formation in AX4 (data not shown). After the tips are
430 established, the slugs/ fruiting bodies move away from ammonia, reflecting a process by which
431 fruiting bodies position themselves from other structures to increase the possibility of spore
432 dispersal (Kosugi and Inouye, 1989). A gaseous signal can act over long distances in a short time
433 and for instance ammonia promotes synchronous development in a colony of yeast cells
434 (Palková et al., 1997; Palková and Forstova, 2000). The slug tip is known to release ammonia
435 probably favouring synchronized development of the entire colony of *Dictyostelium*. However,
436 after the tips are established ammonia exerts negative chemotaxis probably helping the slugs to
437 move away from each other ensuring equal spacing of the fruiting bodies (Feit and Sollitto,
438 1987). Taken together, these findings suggest that ammonia acts as both a local and long-range
439 regulatory signal, integrating environmental and cellular cues to coordinate multicellular
440 development.

441 Cells carrying high ATP, its derivatives cAMP (Bagorda et al., 2009; Singer et al., 2019) and
442 adenosine (Schaap and Wang, 1986), end up in the tip (Hiraoka et al., 2022). Further, 5'-
443 nucleotidase promoter activity is high in pstAB cells (Ubeidat et al., 2002) that significantly
444 covers the tip region suggesting high adenosine levels in the tip. However, extracellular 5'-AMP
445 can be derived from multiple sources such as hydrolysis of cAMP, ATP and RNA (Carpousis et
446 al., 1999).

447 In *adgf* mutants, ammonia levels may not be sufficient enough to neutralize the acidic vesicles
448 and hence, NR staining is intense in the pst region and the ALCs (Bonner, 1952). Ammonia has

449 been shown to differentially suppress cAMP chemotaxis in ALC and pst cells in *Dictyostelium*
450 (Feit et al., 2001).

451 **Ammonia's effect on cAMP signaling in *Dictyostelium***

452 Exposing the cells to ammonia is known to increase intracellular cAMP levels in *D. discoideum*
453 (Riley and Barclay, 1990; Feit et al., 2001), but Schindler and Sussman, (1977) and Williams et
454 al., (1984) reported that high ammonia levels inhibit the synthesis and release of cAMP.
455 However, these experiments use ammonium carbonate (Schindler and Sussman, 1977), or
456 ammonium chloride (Williams et al., 1984) as a source of ammonia, and the possibility of
457 carbonate and chloride ions interfering with development cannot be ruled out. Ammonia is
458 reported to show no effect on cAMP levels in *D. discoideum* slugs (Schaap et al., 1995), but in *D.*
459 *mucoroides,* high ammonia levels are known to block the production of extracellular cAMP. The
460 effect of ammonia on aggregation seems to be species specific notably in *P. violaceum, P.*
461 *pallidum, and D. mucoroides* resulting in wider aggregation territories, while it was not observed
462 in other species such as *D. discoideum* and *D. purpureum* (Bonner and Hoffman, 1963).

463 Adenylate cyclase (AC) activity is regulated by various factors (Steer, 1975). At physiological
464 levels, ammonium ions increase AC activity in the rat brain by 40% (Yeung et al., 1989), but
465 lowered its activity in the liver by about 30% (Wiechetek et al., 1979). Ammonia has been
466 shown to increase the activity of AC-G in *Dictyostelium* sori (Cotter et al., 1999). High ammonia
467 levels by altering the pH, can affect the activity of numerous enzymes whose activity is pH
468 dependent and thus the activity of AC can be impacted by pH variations. *adgf* mutants with low
469 ammonia levels have reduced cAMP levels, and increase in ammonia causes a significant
470 increase in *aca*A expression. In rat brain, ammonia is known to interact with manganese (Rivera-
471 Mancía et al., 2012; Lu et al., 2020), that is known to increase *aca*A expression in *Dictyostelium*

472 (Loomis et al., 1979; Khachatrian et al., 1987). Possibly, ammonia interacts with metal ions like
473 manganese to form 'ammine complexes' (Lipkowski and Galus, 1973), particularly in aqueous
474 environments or under specific conditions where the appropriate ligands are available, and
475 enhances cAMP levels, thus rescuing the mound defects of the mutant.
476 Tip organizer development in *Dictyostelium* depends on the differentiation and appropriate
477 sorting of pst and psp cells (Kay et al., 1978; Williams et al., 1989; Saxe et al., 1993; Williams,
478 2006), a process that relies on signaling of different morphogens including cAMP, adenosine,
479 DIF and ammonia (Bloom and Kay, 1988; Williams, 1988; Riley and Barclay, 1990; Gross,
480 1994). These morphogens modify one another's effects, and determine the choice of the
481 differentiation pathway as well as the spatial arrangement of cells (Bloom and Kay, 1988). Thus,
482 the rescue of the *adgf* mutant upon exposure to ammonia is likely due to cAMP signaling and
483 cell-cell contact.

484 **Possible reasons for reduced cAMP levels in the *adgf* mutant**

485 Higher *pde4* and reduced *acaA* expression may result in low cAMP levels in the mutant. ADA
486 significantly regulates adenosine levels, thus reducing the activation of adenosine-mediated
487 receptors (Van Haastert, 1983). Two classes of adenosine receptors including adenosine alpha-
488 and beta-receptors are known to be expressed in *Dictyostelium* (Theibert and Devreotes, 1984).
489 When adenosine concentrations are high, beta-receptors bound with adenosine inhibit the
490 binding of cAMP to its receptors, thereby inhibiting cAMP signaling (Newell, 1982; Van
491 Haastert, 1983; Theibert and Devreotes, 1984). High adenosine levels in the *adgf* mutant may
492 also reduce cAMP levels via a similar mechanism.

493 The mound/slug tip is believed to carry high adenosine levels restricting additional tip formation
494 (Wang and Schaap, 1985), and our results also suggest that *adgf*$^{-}$ cells with high adenosine end
495 up as pst cells.

496 **Distorted cAMP waves in mutant**

497 Collective cell movement within mounds is essential for cell sorting and the progression from
498 mounds to finger structures (Kellerman and McNally, 1999). In WT mounds, cAMP waves
499 propagate as spirals, while in the mutants, the wave propagation was in concentric circles.
500 Initially, the cAMP waves arise as concentric circles, that, upon symmetry breaking, form spiral
501 waves (Siegert and Weijer, 1995). With successive wave propagation, the circular ring distorts,
502 and one end curls towards the pulsatile center, creating a spiral wave around the organizing
503 center. In *adgf* mutants, however, defective cAMP relay prevents this transition. A surge in
504 phosphodiesterase inhibition is thought to regulate this shift from concentric to spiral wave
505 propagation (Palsson and Cox, 1996), and indeed the phosphodiesterase expression was higher in
506 the *adgf* mutant possibly distorting the wave propagation.

507 The mound/slug tip of *Dictyostelium* generates cAMP pulses (Traynor et al., 1992), and is
508 known to suppress additional tip formation (Farnsworth, 1973). Adenosine, that inhibits
509 additional tip formation represses *pde4* expression whereas ammonia, that promotes tip
510 elongation, increases *pde4* expression. Thus, the restoration of cAMP signaling and spiral wave
511 propagation possibly leads to the rescue of the *adgf*$^{-}$ mound arrest phenotype upon exposure to
512 ammonia. Surprisingly adenosine exerts little effect on tip development in WT cells and studies
513 of Inouye (1989) also reinforce our observations, showing that adenosine does not significantly
514 influence the conversion of pst to psp cells in shaking culture conditions.

515 A robust cAMP relay is required for the transition from concentric to spiral wave propagation,
516 with the corresponding changes in adenylate cyclase or phosphodiesterase activity (Siegert and
517 Weijer, 1995; Palsson and Cox, 1996). Reduced *acaA* expression in the mutant could bias the
518 wave propagation toward concentric rather than spiral geometry. However, further experiments
519 will be required to ascertain this link.

520 **Adenosine deamination drives tip organizer development**

521 A crucial evidence supporting that adenosine deamination is singularly responsible for the rescue
522 of *adgf* $^{-}$ mound arrest comes from experiments where partitioned dish with buffered solution
523 containing adenosine on one side, and the mutants on the other half of the dish. Addition of ADA
524 to the buffer containing adenosine resulted in *adgf* mutants forming tipped mound. Although
525 ammonia's role in *Dictyostelium* development is well established, this report is the first to show a
526 novel role of ammonia in tip development. If natural variants of *Dictyostelium* that fail to form
527 tips exist in soil ecosystems, it is conceivable that these strains could still form fruiting bodies
528 when in proximity to WT strains. This interaction would likely occur through volatile signals
529 such as ammonia diffusing through the shared environment. These diffusible signals may help
530 rescue or coordinate developmental processes among neighbouring cells. Notably, the
531 development of an organism in its natural environment is strongly influenced by volatile
532 compounds present in its surroundings (Schulz-Bohm et al., 2017).

533 **ADA in organizer development and gastrulation in vertebrates**

534 *ada/adgf* expression is found to be high during gastrulation stages in several vertebrates (Pijuan-
535 Sala et al., 2019; Tyser et al., 2021), and collective cell migration during gastrulation and
536 collective cell movement within the *Dictyostelium* mound are remarkably similar (Weijer, 2009),
537 suggesting an overlooked role of ammonia in organizer development. The human homologue of

538 *adgf*, CECR1, is a potential gene for the genetic disorder, Cat-eye syndrome and thus,
539 *Dictyostelium* may also serve as a model to study this condition. Ammonia is crucial in
540 regulating differentiation, metabolism, and gene expression (Stein et al., 2013; Liu et al., 2022).
541 Ammonium has been shown to induce aberrant blastocyst differentiation, disrupt normal
542 metabolic processes, alter pH regulation, and subsequently affect fetal development in mice
543 (Lane and Gardner, 2003). Newt *Triturus* exposed to ammonia shows dorsalization of the ventral
544 marginal zone highlighting the capacity of ammonia to alter embryonic axis formation (Yamada,
545 1950). Furthermore, research on avian embryos has revealed significant ammonia content in
546 developing eggs, suggesting a potential role for ammonia in the energy metabolism during
547 ontogenesis (Needham, 1926). While this raises the possibility of conserved mechanisms, further
548 studies will be needed to determine whether adenosine deamination plays a role in organizer
549 development across different systems.

550 ***dhkD* functions upstream of *adgf***

551 The histidine kinase *dhkD*, a member of the two-component family of histidine kinases, appears
552 to function upstream of *adgf*, adding to our understanding of the signaling cascade in
553 *Dictyostelium*. Histidine kinases play essential roles in regulating developmental transitions, with
554 *dhkC*, for example, initiating the late developmental program that ultimately leads to fruiting
555 body formation (Singleton et al., 1998). This function of *dhkC* is regulated in part by ammonia
556 levels, as low ammonia concentrations have been shown to inhibit the *dhkC* phospho-relay,
557 thereby influencing the developmental outcomes (Kirsten et al., 2005). In *Dictyostelium*, several
558 histidine kinases, including *dhkA*, *dhkB*, *dhkC*, and *dokA*, coordinate cAMP signaling to
559 modulate the activity of PKA, a cAMP-dependent protein kinase that is essential for proper

560 development (Anjard and Loomis, 2003). These findings suggest the interdependencies within
561 the signaling network in regulating multicellular development in *Dictyostelium.*

562 **Model of ADGF action**

563 Ammonia generated from multiple sources is likely to be quenched rapidly by the intracellular
564 acidic vesicles of pst cells, increasing its pH and favoring collective cell movement driving
565 mound/ slug tip development. However, the slime sheath at the back of the slug may prevent the
566 diffusion of ammonia, and thus the major route of ammonia emission will be from the slug front
567 (Farnsworth and Loomis, 1974). Although ammonia is likely to be formed from several sources
568 in *Dictyostelium*, a critical threshold concentration of ammonia may be necessary for tip
569 development. The failure of even one pathway may result in a drop-in ammonia levels, exerting
570 an effect on development (Figure 11). Thus, ammonia is likely to be important for the maturation
571 of tip cells.

572 Our study shows that *adgf* acts downstream of *dhkD* and *in silico* studies have shown that *dhkD*
573 interacts with *adgf*. Therefore, it is likely that in the presence of ammonia, *dhkD* activates the
574 phosphorelay, in turn increasing intracellular cAMP levels, leading to tip formation. Histidine
575 kinase *dhkC* is known to phosphorylate *regA* in *Dictyostelium* (Thomason et al.,1999). However,
576 based on docking we found no direct interaction of *regA* with ADGF (data not shown). Thus, the
577 integration of histidine kinase signaling ensures coordinated multicellular organization in
578 *Dictyostelium* (Aoki et al., 2020). Previous work in other systems have found ADA to be
579 interacting with CD 26 (dpp IV) (Tanaka et al., 1993), and docking DdADGF with AprA (dpp8)
580 also supports this observation. However, adding ADA inhibitor to *aprA* mutant (dpp8), showed
581 no effect on the phenotype (data not shown).

582 **Supplementary Results**

583 **Genes involved in autophagy and tipped mound formation do not show altered expression**
584 **in the *adgf* mutant**

585 Autophagy helps in maintaining cellular homeostasis by promoting the breakdown of damaged
586 proteins and organelles (Mizushima et al., 2008), and ammonia is recognised to be a diffusible
587 regulator of autophagy in human cells (Eng et al., 2010). To investigate if autophagy is impaired
588 in the mutant, the expression of autophagy markers *atg8* and *atg18* were examined and there was
589 no discernible change in the expression levels when compared to WT. The tipless to tipped
590 mound transition as well as late developmental gene expression is regulated by *gbf*A, a G-box
591 binding factor (GBF). However, in the *adgf* mutant the *gbf*A expression levels were comparable
592 with no significant difference between the WT at 16 h (data not shown). Without the assay for
593 autophagy as well as assay for GBF activity, these expression studies alone are not conclusive to
594 rule out the role of these factors in tip formation.

595 **ADA does not deaminate cytokinin**

596 ADA is known to interact with 5'AMP (Hanif et al., 2022) and in *Dictyostelium*, 5′-AMP serves
597 as a direct precursor of cytokinin, playing a significant role in cellular signaling and development
598 (Taya et al., 1978). Although docking studies suggest low to moderate binding of ADGF with
599 cytokinins (zeatin, dihydrozeatin, isopentenyl adenine), we carried a functional assay by mixing
600 cytokinin and ADA with KK2 buffer in one side of the Petridish and found no rescue of the
601 mutant in such conditions (data not shown), suggesting no functional activity between ADA and
602 the versions of cytokinin tested.

603 **Supplementary discussion**

604 **Plausible routes of caffeine action rescuing the mound arrest phenotype**

605 The *adgf* mound arrest could be rescued by the addition of the adenosine antagonist, caffeine but
606 treatment with the *pde4* inhibitor, IBMX failed to rescue the mound arrest. Caffeine is known to
607 reduce adenosine levels in blood plasma (Conlay et al., 1988) and also increase ammonium
608 levels in urine samples of rabbits (Bernheim and Bernheim, 1945). Thus, the mound rescue upon
609 caffeine treatment may be a result of reduced adenosine and increased ammonia levels. With
610 respect to caffeine action on cAMP levels, the reports are contradictory. Caffeine has been
611 reported to increase adenylate cyclase expression thereby increasing cAMP levels (Hagmann,
612 1986) whereas Alvarez-Curto et al., (2007) found that caffeine reduced intracellular cAMP levels
613 in *Dictyostelium*. Although, caffeine is moderately potent in inhibiting PDE enzyme activity, the
614 *in vivo* concentrations are likely to be low to be associated with effective PDE inhibition (Burg
615 and Werner, 1975; Daly, 1993).

616 **Material and Methods**

617 **Bioinformatic analyses of ADGF**

618 The genomic sequence and the protein sequence of ADGF were obtained either from dictybase
619 (http://dictybase.org) or NCBI database (https://www.ncbi.nlm.nih.gov/). The ADA domain
620 within the DdADGF was identified by SMART and BLAST (http://smart.embl-heidelberg.de/)
621 (https://blast.ncbi.nlm.nih.gov/Blast.cgi) (Altschul et al., 1990; Letunic and Bork, 2018) analyses.
622 A phylogenetic tree was generated by aligning multiple amino acid sequences of ADGF from
623 several taxa. Neighbour Joining approach and the MUSCLE alignment tool of the MEGAX
624 programme were used for constructing the tree (Saitou and Nei, 1987). The tertiary structure of
625 ADGF was obtained using the online programme alphafold (https://alphafold.ebi.ac.uk/) (Jumper
626 et al., 2021), and PyMol was used for viewing the images. The expression profiles of *ada* and

627 *ada2* during mouse and human gastrula development were retrieved from the
628 marionilab.cruk.cam.ac.uk/MouseGastrulation2018/ and human-gastrula.net/ databases (Pijuan-
629 Sala et al., 2019; Tyser et al., 2021), respectively. Protein-protein docking was carried out using
630 High Ambiguity Driven Protein-Protein Docking (HADDOCK) version 2.4.

631 **Culture and development of *Dictyostelium discoideum***

632 *D. discoideum* (WT-AX4) cells or the mutant *adgf* derived from AX4, (DBS0237637) were
633 cultured in modified maltose-HL5 medium (Formedium, UK) with 100,000 U/L penicillin and
634 0.1 g/L streptomycin. Three independent mutants (GWDI_17_D_7, GWDI_47_C_1,
635 GWDI_132_H_3; insertion in exon 2 in all three mutants) of the *adgf* gene (DDB_G0275179)
636 were obtained from the GWDI bank (https://remi-seq.org), in *Dictyostelium* stock centre, North
637 Western University, USA (Gruenheit et al., 2021). The mound defects were identical in all three
638 and strain GWDI_47_C_1 alone was characterised further. The culture was raised as a
639 monolayer in Petri plates or grown in an Erlenmeyer flask in shaking conditions at 150 rpm and
640 22 °C, to a cell density of 2-4x10^6 cells/ml. The cells were also grown on SM/5 agar plates
641 supplemented with *Klebsiella pneumoniae* at 22 °C (2 g/L glucose, 2 g/L protease peptone, 0.4
642 g/L yeast extract, 1 g/L $MgSO_4.H_2O$, 0.66 g/L K_2HPO_4, 2.225 g/L KH_2PO_4, 1% Bactoagar, pH
643 6.4). For developmental assays, freshly starved cells were washed twice with ice cold KK2
644 buffer (2.25 g KH_2PO_4 and 0.67 g K_2HPO_4 per litre, pH 6.4), and plated on 1% non-nutrient
645 KK2 agar plates at a density of 5x10^5 cells/cm^2 (Nassir et al., 2019). Thereafter, the plates were
646 incubated in dark conditions at 22 °C for development.

647 ***Dictyostelium* genomic DNA isolation**

648 WT and *adgf*$^-$ cells grown axenically were harvested, and the pellet was resuspended in 1 ml of
649 lysis buffer (50 mM Tris-Cl, pH 8; 10 mM EDTA; 0.8% SDS). To this mixture, 200 µl of

650 Nonidet P-40 (NP40), a non-ionic detergent, was added, vortexed and centrifuged at 12,000 g for
651 15 min at room temperature (RT). The resultant pellet was gently vortexed, resuspended in 500
652 µl of lysis solution containing 200 µg/ml Proteinase K, and incubated at 65 °C for 30 min. 300 µl
653 of phenol: chloroform was added to this suspension, centrifuged at 18,000 g for 10 min at RT,
654 and the resultant aqueous phase was extracted carefully. An equal amount of chloroform was
655 added and centrifuged at 18,000 g for 10 min at RT. Following this, 750 µl of pure ethanol was
656 added to the suspension, which was then centrifuged at 12,000 g for 15 min at 4 °C. Genomic
657 DNA was precipitated by adding twice the volume of absolute ethanol and 1/10th the volume of 3
658 M sodium acetate. After a 10 min centrifugation at 15,000 g, the pellet was cleaned using 70%
659 ethanol and stored at 4 °C. Electrophoresis was conducted in TAE buffer at 50 V using a Medox
660 power pack system (India), and the integrity of DNA was confirmed on a 1% agarose gel.

661 **Validation of the *adgf* mutant**

662 To validate the blasticidin (*bs*r) resistance cassette insertion in the *adgf* mutant, WT and *adgf* $^{-}$
663 genomic DNA were isolated, and a diagnostic PCR was performed using the gene and *bsr* insert
664 specific primers in accordance with the guidelines provided in the GWDI website. A qRT-PCR
665 was carried out to confirm the absence of *adgf* expression in the mutant cells. The primers used
666 for mutant validation are listed in Supplementary Table S2.

667 **Quantitative real-time PCR (qRT-PCR)**

668 Total RNA was extracted from WT and *adgf* $^{-}$ cells using Trizol reagent (Favorgen, USA) at
669 specified intervals (every four hours from 0 to 24 h). cDNA was synthesized from the total RNA
670 using a PrimeScript 1st Strand cDNA Synthesis Kit (Takara, Japan). Random primers from the
671 manufacturer were used to generate the cDNA from a template of 1 µg total RNA. qRT-PCR
672 was performed using SYBR Green Master Mix (Thermo Scientific, USA) and 1 µl of cDNA.

673 The expression levels of *adgf*, *acaA*, cAMP receptor A (*carA*), phosphodiesterases (*pdsA*, *regA*),
674 5' nucleotidase (*5'nt*), extracellular matrix A (*ecmA*), extracellular matrix B (*ecmB*), prespore A
675 (*pspA*), countin (*ctn*), and small aggregate (*smlA*) were quantified with a QuantStudio Flex 7
676 (Applied Biosystems, USA). The mitochondrial large RNA subunit (*rnlA*) served as an internal
677 control. qRT-PCR data analysis was conducted according to the method described by Schmittgen
678 and Livak (2008). The primer sequences used for qRT-PCR are provided in Supplementary
679 Table S4.

680 **Generation of *adgf* over expression construct**

681 The full-length 1.7 kb *adgf* sequence was PCR-amplified using ExTaq polymerase (Takara,
682 Japan) with WT genomic DNA as the template. The amplified product was then ligated into the
683 pDXA-GFP2 vector at the HindIII and KpnI restriction sites. Both *adgf* $^{-}$ and WT cells were
684 electroporated with this vector, and G418-resistant clones (10 µg/ml) were isolated for further
685 analysis. The expression of *adgf* was confirmed by semi-quantitative PCR. The corresponding
686 primer sequences are listed in Supplementary Table S3.

687 **Transformation of *Dictyostelium discoideum***

688 WT and *adgf* $^{-}$ cells grown axenically were harvested, washed twice with ice-cold EP buffer (10
689 mM KH_2PO_4, 10 mM K_2HPO_4, 50 mM sucrose, pH 6.2), and resuspended in 100 µl of EP++
690 solution (10 K_2HPO_4 mM, 10 mM KH_2PO_4, 50 mM sucrose, 1 mM $MgSO_4$, 1 mM $NaHCO_3$, 1
691 mM ATP, 1 µM $CaCl_2$) containing 10 µg of plasmid vector (Nassir et al., 2019) in pre-cooled
692 cuvettes (BioRad, USA). The cells were electroporated using a BTX ECM830 electroporator
693 (Harvard Apparatus, USA) at 300 V with 2 ms pulses and five square wave pulses at 5-second
694 intervals. The cells were then transferred to a Petri dish with 10 ml of HL5 medium and

695 incubated at 22 °C. After 24 hours, G418 (10 µg/ml) was added to the medium, and resistant
696 colonies were selected for further analysis.

697 **Preparation of conditioned media (CM)**

698 WT and *adgf* $^{-}$ cells grown in HL5 medium were collected at the mid-log (ML) phase,
699 resuspended in KK2 buffer at a density of $1x10^7$ cells/ml, and incubated at 22 °C with shaking
700 for 20 hours. The clarified supernatant obtained after centrifugation was used for the experiments.

701 **Assay for ADA activity**

702 Total ADA activity from *Dictyostelium* was determined as per the protocol of the manufacturer
703 (Abcam, USA; Cat No: ab204695). For sample preparation, $5x10^5$ cells/cm^2 were seeded onto
704 KK2 agar plates and at the mound stage, ice cold ADA assay buffer was flooded, then vigorously
705 pipetted to disrupt the mound integrity. The cell homogenate was agitated on a rotary shaker at
706 4 °C for 15 min and then centrifuged at 12,000 rpm for 10 min in a cold microfuge tube. The
707 supernatant was subjected to the ADA assay. This ADA test relies on adenosine to inosine
708 formation. The intermediate formed combines with the probe to produce uric acid, which is
709 quantified at 293 nm. BCA (Bicinchonic acid) assay kit (Thermoscientific, USA) was used for
710 determining the protein concentration. One unit of ADA activity is defined as the amount of
711 enzyme that hydrolyses adenosine to yield 1 µmol of inosine per min under the assay conditions.

712 **Adenosine quantification**

713 Total adenosine levels from *Dictyostelium* mounds were measured according to the
714 manufacturer's protocol, using the adenosine assay kit (Abcam, USA; Cat No: ab211094). Cells
715 grown in HL5 were collected, washed and plated on KK2 agar plates. The cell lysis buffer was
716 added to the plates with mounds and mixed thoroughly. 50 µl of the lysate was mixed with 2 U

717 of ADA and was subjected to incubation for 15 min at RT. Adenosine quantification involves the
718 use of ADA and after a series of enzymatic reactions, an intermediate is formed which reacts
719 with the adenosine probe generating a fluorescent product. Using a spectrofluorometer (Perkin
720 Elmer, USA; λEx = 544 nm/λEm = 590), the fluorescence intensity was measured, which is
721 proportional to the concentration of adenosine. The adenosine levels were quantified using the
722 adenosine standard curve.

723 **Quantification of ammonia**

724 Ammonia assay kit (Sigma-Aldrich, USA; Cat No: AA0100) was used for estimating the total
725 ammonia levels. WT and *adgf* $^{-}$ cells developed on KK2 agar plates were sealed with parafilm
726 and incubated at 22 °C. The mounds were collected using lysis solution, and the debris was
727 removed by centrifugation at 10,000 g for 10 min. The supernatant was used for further analysis.
728 For the ammonia assay, 1 ml of assay reagent was mixed thoroughly with either 100 µl of
729 samples or standards, incubated for 5 min at RT, and the absorbance was measured at 340 nm.
730 Then, 10 µl of L-glutamate dehydrogenase (GDH) solution was added to each cuvette, and after
731 a 5-min incubation at 25 °C, the absorbance was measured again at 340 nm using a
732 spectrophotometer (Eppendorf, Germany). In the presence of GDH, ammonia combines with α-
733 ketoglutaric acid and reduced NADPH to produce L-glutamate and oxidised $NADP^{+}$. The
734 decrease in absorbance at 340 nm is proportional to the ammonia concentration. The ammonia
735 standard curve was used to calculate the ammonia levels.

736 **Volatile ammonia generation**

737 To generate ammonia, 1 ml of 1 N NaOH and 1 ml of NH_4Cl (concentrations used 0.1 mM, 1
738 mM, 10 mM) were mixed thoroughly (Thadani et al., 1977; Feit et al., 1990) and from this mix,
739 2 ml was aliquoted in the upper half of the Petri dish. The other half of the plate with the *adgf* $^{-}$

740 mounds on KK2 agar were inverted, sealed and incubated at 22 °C. To determine whether WT
741 mounds, physically separated from the mutants could rescue the mound arrest, WT ($1x10^6$
742 cells/cm^2) and *adgf* $^-$ ($5x10^5$ cells/cm^2) cells were developed on KK2 agar plates on either side of
743 compartmentalised and sealed Petri plates. *adgf* $^-$ cells developed on either side of the dish
744 served as controls.

745 **Quantification of cAMP**

746 Using the cAMP-XP test kit and following the manufacturer's instructions, total cAMP levels
747 were determined from both the WT and the mutant (Cell signaling, USA). WT and *adgf* $^-$
748 mounds were disrupted and collected in 1 ml ice cold KK2 buffer. After centrifuging the pellet,
749 100 µl of 1X lysis solution was added, and the mixture was incubated in ice for 10 min.
750 Subsequently, 50 µl of lysate and 50 µl of HRP-conjugated cAMP solution were added to the test
751 plates, which were then shaken horizontally at RT. After 3 h incubation, the wells were emptied
752 and washed three times with 200 µl of 1X wash buffer. 100 µl of stop solution was added to halt
753 the reaction, and the absorbance was measured at 450 nm using a spectrophotometer (Biorad,
754 USA). The cAMP standard curve was used to determine the cAMP levels.

755 **Visualisation of cAMP waves using dark field optics**

756 $5x10^5$ cells/cm^2 were developed on KK2 agar plates under moist, dark conditions to monitor the
757 propagation of cAMP waves. Using a Nikon DS-5MC camera mounted on a Nikon SMZ-1000
758 stereo zoom and Nikon Eclipse TE2000 inverted microscope, a time-lapse video of the
759 aggregation was captured in real-time (Nikon, Japan). cAMP optical density waves were
760 displayed by subtracting the image pairs (Siegert and Weijer, 1995) after processing the images
761 with the NIS-Elements D program or ImageJ (NIH, USA).

762 **Under agarose cAMP chemotaxis assay**

763 The under-agarose cAMP chemotaxis assay (Woznica and Knecht, 2006; Singh and Insall, 2022)
764 was carried out with cells obtained from WT and *adgf* $^{-}$ mounds. Briefly, the cells were starved
765 in KK2 buffer at $1x10^7$ cells/ml density. Three parallel troughs, each measuring 2 mm in width,
766 were set up on a Petri dish containing 1% agarose. In the outer two troughs, 100 µl of WT and
767 *adgf* $^{-}$ cell suspension was aliquoted respectively and 10 µM cAMP was added to the central
768 trough. Cell migration toward cAMP was recorded every 30 s over a total duration of 20 min
769 using the NIS-Elements D software and an inverted Nikon Eclipse TE2000 microscope (Nikon,
770 Japan). 35 cells were tracked each time and subsequently analysed using ImageJ (NIH, USA).

771 **Mixing WT with mutant cells**

772 WT and *adgf* $^{-}$ cells cultured in HL5 medium, were harvested at the mid log (ML) phase by
773 centrifugation, rinsed twice with ice-cold KK2 buffer. The cells mixed in different ratios (1:9,
774 2:8 and 1:1) were adjusted to a final density of $5x10^5$ cells/cm^2, plated on 1% KK2 agar plates,
775 and incubated at 22 °C for development.

776 **Tracking cell fate after mixing**

777 *Dictyostelium* cells harvested from fresh HL5 media were resuspended at a density of $1x10^6$
778 cells/ml in KK2 buffer, followed by incubation at 22 °C for 1.5 h in shaking conditions with 0.2
779 µM DIL (Invitrogen, USA). DIL has been used extensively as a cell tracker in *C. elegans*,
780 *Xenopus and* mice (Schultz and Gumienny, 2012; Xu et al., 2020; Erdogan et al., 2016). WT or
781 *adgf* $^{-}$ cells labelled with DIL were mixed with the unlabelled cells in a ratio of 1:9, 2:8 and 1:1
782 and plated for development. In the ratios mentioned, the smaller fraction represents the stained
783 cells. DIL is a lipophilic dye that selectively stains the plasma membranes of living cells,
784 allowing visualization and analysis of cell morphology.

785 **Neutral red staining of mounds and slugs**

786 WT and *adgf* $^{-}$ cells harvested from HL5 cultures were resuspended at a density of $1x10^7$ cells
787 per ml in KK2 buffer and treated with 0.005% neutral red (NR) solution for 15 min at RT in
788 shaking conditions (Bonner, 1952). The stained cells were washed twice with KK2 buffer, plated
789 on buffered agar plates and thereafter, NR stained slugs were observed using an upright
790 microscope.

791 **Cell-type specific expression analysis of *adgf***

792 To determine the differential expression of *adgf,* if any, between the two major cell types, psp-
793 GFP cells in AX4 background were developed on KK2 agar plates at a density of 5×10^5
794 cells/cm² until they reached the slug stage, as described by Ratner and Borth (1983).
795 Fluorescence was initially monitored using microscopy to confirm GFP expression. Slugs were
796 then dissociated in 20 mM phosphate buffer containing 40 mM EDTA, pH 7.0 (Nadin et al.,
797 2000), filtered through a 10-µm nylon mesh, chilled on ice, and using FACS (FACS Discover S8
798 Image Sorter (BD Biosciences, USA)) the two cell types were sorted. Sorting was performed at a
799 rate of 10,000 cells/s with a 488 nm laser. GFP-positive prespore (psp) cells and GFP-negative
800 prestalk (pst) cells were collected separately on ice over several hours. Total RNA was extracted
801 from both cell populations, and the expression of *adgf* was analyzed using RT-PCR.

802 **Cell-cell adhesion assay**

803 After 14 h of development on phosphate buffered agar plates, WT and *adgf* $^{-}$ mounds were
804 disaggregated by repeated pipetting and vortexing using ice-cold KK2 buffer. Dissociated cells
805 were resuspended in KK2 buffer and incubated at 150 rpm for 45 min. Single and non-adherent
806 cells were counted using a Neubauer chamber (Lam et al., 1981).

807 **Treatment of *Dictyostelium* cells with different compounds**

808 A highly specific ADA inhibitor, DCF that inhibits both extra and intra-cellular ADAs (Cha et
809 al., 1975) was mixed with the WT cell suspension and plated on 1% non- nutrient KK2 agar
810 plates at a density of $5x10^5$ cells/cm^2. Of the different DCF concentrations tested (10 nM, 50 nM,
811 100 nM and 1 μM), 100 nM showed complete tip inhibition.

812 For the enzymatic rescue assay, 10 U of bovine ADA dissolved in KK2 buffer (Sigma-Aldrich,
813 USA) was added onto mutant mounds. The concentrations of 8-Br-cAMP (2 mM), cAMP (0.1
814 mM, 0.5 mM), c-di-GMP (0.1 mM, 0.5 mM), adenosine (1 μM, 10 μM, 100 μM, 1 mM),
815 caffeine (10 nM, 100 nM, 1 μM) and IBMX (0.5 mM) were based on previous publications
816 (Chen et al., 2017; Chen and Schaap, 2012; Nassir et al., 2019; Siegert and Weijer, 1989) and
817 these compounds were added independently either on top of the mounds or supplemented while
818 plating. All the fine chemicals were from Sigma-Aldrich, USA except when mentioned.

819 **Microscopy**

820 Microscopy was performed using a Nikon SMZ-1000 stereo zoom microscope with
821 epifluorescence optics, Nikon 80i Eclipse upright microscope, or a Nikon Eclipse TE2000
822 inverted microscope, connected with a digital sight DS-5MC camera (Nikon). Image processing
823 was carried out using NIS-Elements D (Nikon) or Image J.

824 **Statistical tools**

825 Data analyses were carried out using Microsoft Excel (2016). Statistical significance was
826 determined by paired or unpaired, two-tailed Student's t-test and ANOVA analysis (GraphPad
827 Prism, version 7).

828 **Acknowledgements**

829 We gratefully acknowledge the help of NBRP Nenkin, Japan and *Dictyostelium* Stock Center
830 (DSC), Northwestern University, USA for providing various strains and plasmids used in this
831 study. We thank Prof. Richard Gomer, Texas A&M, USA for providing *aprA* mutant strain. We
832 thank Prof. Kei Inouye, Kyoto University, Japan, Prof. Kees Weijer, University of Dundee, UK
833 and Prof. Gad Shaulsky, Baylor College of Medicine USA for their comments on an earlier
834 version of the manuscript/ thesis. We acknowledge Dr. Srividhya, Facility-in-Charge, Flow
835 Cytometry facility, Bio-SAIF, IIT Madras, for assistance with FACS and technical support. We
836 gratefully acknowledge the help from Indian Council of Medical Research (ICMR), New Delhi
837 for their support in this project. We thank Steve Hawthorne from Scholarly memory for his
838 feedback and suggestions on an earlier version of the manuscript.

839 **Author contributions**

840 P.H. and R.B. conceptualized the work. P.H. performed all experiments. P.H. and R.B. analysed
841 the data and wrote the manuscript.

842 **Competing interests**

843 The authors declare no competing interests.

844 **References**

845 Aoki, M. M., Emery, R. J., Anjard, C., Brunetti, C. R., and Huber, R. J. (2020). Cytokinins in
846 *Dictyostelia*–A unique model for studying the functions of signaling agents from species to
847 kingdoms. *Frontiers in Cell and Developmental Biology*, 511.

848 Altschul, S. F., Gish, W., Miller, W., Myers, E. W. and Lipman, D. J. (1990). Basic local
849 alignment search tool. *J. Mol. Biol.* 215, 403–410.

850 Alvarez-Curto, E., Weening, K. E., and Schaap, P. (2007). Pharmacological profiling of the
851 *Dictyostelium* adenylate cyclases ACA, ACB and ACG. *Biochemical Journal*, 401(1), 309-316.

852 Anjard, C., and Loomis, W. F. (2003). Histidine kinases of *Dictyostelium*. In *Histidine Kinases*
853 *in Signal Transduction* (pp. 421-438). Academic Press.

854 Bader, S., Kortholt, A., and Van Haastert, P. J. (2007). Seven *Dictyostelium discoideum*
855 phosphodiesterases degrade three pools of cAMP and cGMP. *Biochemical Journal*, 402(1), 153-
856 161.

857 Bagorda, A., Das, S., Rericha, E. C., Chen, D., Davidson, J., and Parent, C. A. (2009). Real-time
858 measurements of cAMP production in live *Dictyostelium* cells. *Journal of Cell Science*, 122(21),
859 3907-3914.

860 Bernheim, F., and Bernheim, M. L. (1945). Note on the effect of caffeine on ammonia and urea
861 excretion in rabbits. *American Journal of Physiology-Legacy Content*, 145(1), 115-117.

862 Bloom, L., and Kay, R. R. (1988). The search for morphogenes in *Dictyostelium*. *Bioessays*, 9(6),
863 187-191.

864 Bonner, J. T. (1952). Morphogenesis: an essay on development (Vol. 28). Princeton, NJ:
865 Princeton University Press.

866 Bonner, J. T., and Hoffman, M. E. (1963). Evidence for a substance responsible for the spacing
867 pattern of aggregation and fruiting in the cellular slime molds. *Development*, 11(3), 571-589.

868 Bonner, J. T., Suthers, H. B., and Odell, G. M. (1986). Ammonia orients cell masses and speeds
869 up aggregating cells of slime moulds. *Nature*, 323(6089), 630-632.

870 Bonner, J. T., Chiang, A., Lee, J., and Suthers, H. B. (1988). The possible role of ammonia in
871 phototaxis of migrating slugs of *Dictyostelium discoideum*. *Proceedings of the National*
872 *Academy of Sciences (USA)*, 85(11), 3885-3887.

873 Bonner, J. T., Har, D., and Suthers, H. B. (1989). Ammonia and thermotaxis: further evidence
874 for a central role of ammonia in the directed cell mass movements of *Dictyostelium discoideum*.
875 *Proceedings of the National Academy of Sciences (USA)*, 86(8), 2733-2736.

876 Bradbury, J. M., and Gross, J. D. (1989). The effect of ammonia on cell-type-specific enzyme
877 accumulation in *Dictyostelium discoideum*. *Cell Differentiation and Development*, 27(2), 121-
878 128.

879 Brock, D. A., and Gomer, R. H. (1999). A cell-counting factor regulating structure size in
880 *Dictyostelium*. *Genes and Development*, 13(15), 1960-1969.

881 Brock, D. A., Ehrenman, K., Ammann, R., Tang, Y., and Gomer, R. H. (2003). Two components
882 of a secreted cell number-counting factor bind to cells and have opposing effects on cAMP
883 signal transduction in *Dictyostelium*. *Journal of Biological Chemistry*, 278(52), 52262-52272.

884 Burg, A. W., and Werner, E. (1975). Effect of orally-administered caffeine and theophylline on
885 tissue concentrations of 3', 5'cyclic-amp and phospho-diesterase. *Federation Proceedings,* 34(3),
886 332-332.

887 Carpousis, A. J., Vanzo, N. F., and Raynal, L. C. (1999). mRNA degradation: a tale of poly (A)
888 and multiprotein machines. *Trends in Genetics*, 15(1), 24-28.

889 Carrin, I., Murgia, I., McLachlan, A., and Kay, R. R. (1996). A mutational analysis of
890 *Dictyostelium discoideum* multicellular development. *Microbiology*, 142(4), 993-1003.

891 Cha, S., Agarwal, R. P., and Parks Jr, R. E. (1975). Tight-binding inhibitors—II: Non-steady
892 state nature of inhibition of milk xanthine oxidase by allopurinol and alloxanthine and of human
893 erythrocytic adenosine deaminase by coformycin. *Biochemical Pharmacology*, 24(23), 2187-
894 2197.

895 Chen, Z. H., and Schaap, P. (2012). The prokaryote messenger c-di-GMP triggers stalk cell
896 differentiation in *Dictyostelium*. *Nature*, 488(7413), 680-683.

897 Chen, Z. H., Singh, R., Cole, C., Lawal, H. M., Schilde, C., Febrer, M., Barton, G. J. and Schaap,
898 P. (2017). Adenylate cyclase A acting on PKA mediates induction of stalk formation by cyclic
899 diguanylate at the *Dictyostelium* organizer. *Proceedings of the National Academy of Sciences*
900 *(USA)*, 114(3), 516-521.

901 Chien, S., Chung, C. Y., Sukumaran, S., Osborne, N., Lee, S., Ellsworth, C., Mc Nally, G. Y.,
902 and Firtel, R. A. (2000). The *Dictyostelium* LIM domain-containing protein LIM2 is essential for
903 proper chemotaxis and morphogenesis. *Molecular Biology of the Cell*, *11*(4), 1275-1291.

904 Cristalli, G., Costanzi, S., Lambertucci, C., Lupidi, G., Vittori, S., Volpini, R., and Camaioni, E.
905 (2001). Adenosine deaminase: functional implications and different classes of
906 inhibitors. *Medicinal Research Reviews*, 21(2), 105-128.

907 Coates, J. C., and Harwood, A. J. (2001). Cell-cell adhesion and signal transduction during
908 *Dictyostelium* development. *Journal of Cell Science*, 114(24), 4349-4358.

909 Conlay, L. A., Evoniuk, G., and Wurtman, R. J. (1988). Endogenous adenosine and hemorrhagic
910 shock: effects of caffeine administration or caffeine withdrawal. *Proceedings of the National*
911 *Academy of Sciences (USA)*, 85(12), 4483-4485.

912 Costenla, A. R., Cunha, R. A., and De Mendonça, A. (2010). Caffeine, adenosine receptors, and
913 synaptic plasticity. *Journal of Alzheimer's Disease*, 20(s1), S25-S34.

914 Cotter, D. A., Dunbar, A. J., Buconjic, S. D., and Wheldrake, J. F. (1999). Ammonium
915 phosphate in sori of *Dictyostelium discoideum* promotes spore dormancy through stimulation of
916 the osmosensor ACG. *Microbiology*, 145(8), 1891-1901.

917 Daly, J. W. (1993). Mechanism of action of caffeine. *Caffeine, coffee, and health*, 97-150. Raven
918 press.

919 Davies, L., Satre, M., Martin, J. B., and Gross, J. D. (1993). The target of ammonia action in
920 *Dictyostelium*. *Cell*, 75(2), 321-327.

921 Dolezal, T., Dolezelova, E., Zurovec, M., and Bryant, P. J. (2005). A role for adenosine
922 deaminase in *Drosophil*a larval development. *PLoS Biology*, 3(7), e201.

923 Eichinger, L et al., (2005). The genome of the social amoeba *Dictyostelium discoideum*. *Nature*.
924 435(7038):43-57.

925 Eidhammer, I., Jonassen, I., and Taylor, W. R. (2000). Structure comparison and structure
926 patterns. *Journal of Computational Biology*, *7*(5), 685-716.

927 Eng, C. H., Yu, K., Lucas, J., White, E., and Abraham, R. T. (2010). Ammonia derived from
928 glutaminolysis is a diffusible regulator of autophagy. *Science signaling*, 3(119).

929 Erdogan, B., Ebbert, P. T., and Lowery, L. A. (2016). Using *Xenopus laevis* retinal and spinal
930 neurons to study mechanisms of axon guidance in vivo and in vitro. *Seminars in Cell and*
931 *Developmental Biology,* 51, 64-72. Academic Press. USA.

932 Farnsworth, P. (1973). Morphogenesis in the cellular slime mould *Dictyostelium discoideum*; the
933 formation and regulation of aggregate tips and the specification of developmental axes.
934 *Development,* 29(2), 253-266.

935 Farnsworth, P. A., and Loomis, W. F. (1974). A barrier to diffusion in pseudoplasmodia of
936 *Dictyostelium discoideum*. *Developmental Biology*, 41(1), 77-83.

937 Feit, I. N. (1988). Ammonia can stimulate or inhibit aggregate density in *Dictyostelium*
938 *mucoroides*: A quantitative test of the hypothesis that ammonia is the aggregation-suppressing
939 gas. *Developmental Genetics*, 9(4-5), 639-652.

940 Feit, I. N., Bonner, J. T., and Suthers, H. B. (1990). Regulation of the anterior-like cell state by
941 ammonia in *Dictyostelium discoideum*. *Developmental Genetics*, 11(5-6), 442-446.

942 Feit, I. N., Medynski, E. J., and Rothrock, M. J. (2001). Ammonia differentially suppresses the
943 cAMP chemotaxis of anterior-like cells and prestalk cells in *Dictyostelium discoideum*. *Journal*
944 *of Biosciences*, 26, 157-166.

945 Feit, I. N., and Sollitto, R. B. (1987). Ammonia is the gas used for the spacing of fruiting bodies
946 in the cellular slime mold, *Dictyostelium discoideum*. *Differentiation*, 33(3), 193-196.

947 Felsenstein, J. (1985). Confidence limits on phylogenies: an approach using the
948 bootstrap. *Evolution*, 39(4), 783-791.

949 Firtel, R. A. (1996). Interacting signaling pathways controlling multicellular development in
950 *Dictyostelium*. *Current Opinion in Genetics and Development*, 6(5), 545-554.

951 Follstaedt, S. C., Kirsten, J. H., and Singleton, C. K. (2003). Temporal and spatial expression of
952 ammonium transporter genes during growth and development of *Dictyostelium*
953 *discoideum. Differentiation*, 71(9-10), 557-566.

954 Gaspar, H. B. (2010). Bone marrow transplantation and alternatives for adenosine deaminase
955 deficiency. *Immunology and Allergy Clinics*, 30(2), 221-236.

956 Gee, K., Russell, F., and Gross, J. D. (1994). Ammonia hypersensitivity of slugger mutants of *D.*
957 *discoideum*. *Journal of Cell Science*, 107(2), 701-708.

958 Godecke, A. (2008). cAMP: fuel for extracellular adenosine formation? *British Journal of*
959 *Pharmacology*, 153(6), 1087-1089.

960 Gruenheit, N. et al., (2021). Mutant resources for functional genomics in *Dictyostelium*
961 *discoideum* using REMI-seq technology. *BMC Biology*, 19(1), 172.

962 Gross, J. D., Bradbury, J., Kay, R. R., and Peacey, M. J. (1983). Intracellular pH and the control
963 of cell differentiation in *Dictyostelium discoideum*. *Nature*, 303(5914), 244-245.

964 Gross, J. D., Peacey, M. J., and Von Strandmann, R. P. (1988). Plasma membrane proton
965 pump inhibition and stalk cell differentiation in *Dictyostelium discoideum*. *Differentiation*,
966 38(2), 91-98.

967 Gross, J. D. (1994). Developmental decisions in *Dictyostelium discoideum*.
968 *Microbiological Reviews*, 58(3), 330-351.

969 Gross, J. D. (2009). Acidic Ca2+ stores, excitability, and cell patterning in *Dictyostelium*
970 *discoideum*. *Eukaryotic Cell*, 8(5), 696-702.

971 Hagmann, J. (1986). Caffeine and heat shock induce adenylate cyclase in *Dictyostelium*
972 *discoideum*. *The EMBO Journal*, 5(13), 3437-3440.

973 Hames, B. D., and Ashworth, J. M. (1974). The metabolism of macromolecules during the
974 differentiation of myxamoebae of the cellular slime mould *Dictyostelium discoideum* containing
975 different amounts of glycogen. *Biochemical Journal*, 142(2), 301-315.

976 Hanif, M. A., Hossen, S., Cho, Y., Sukhan, Z. P., Choi, C. Y., and Kho, K. H. (2022).
977 Characterization and expression analysis of mollusk-like growth factor: A secreted protein
978 involved in Pacific abalone embryonic and larval development. *Biology*, 11(10), 1445.

979 Harrison, M. J. (2005). signaling in the arbuscular mycorrhizal symbiosis. *Annu. Rev. Microbiol*.,
980 59, 19-42.

981 Headrick, J. P., and Willis, R. J. (1989). 5' -Nucleotidase activity and adenosine formation in
982 stimulated, hypoxic and underperfused rat heart. *Biochemical Journal*, 261(2), 541-550.

983 Helgason, T., Daniell, T. J., Husband, R., Fitter, A. H., and Young, J. P. W. (1998). Ploughing up
984 the wood-wide web. *Nature*, 394(6692), 431-431.

985 Hiraoka, H., Wang, J., Nakano, T., Hirano, Y., Yamazaki, S., Hiraoka, Y., and Haraguchi, T.
986 (2022). ATP levels influence cell movement during the mound phase in *Dictyostelium*
987 *discoideum* as revealed by ATP visualization and simulation. *FEBS Open bio*, 12(11), 2042-2056.

988 Honorato, R. V., Koukos, P. I., Jiménez-García, B., Tsaregorodtsev, A., Verlato, M., Giachetti,
989 A., Rosato, A., and Bonvin, A. M. (2021). Structural biology in the clouds: the WeNMR-EOSC
990 ecosystem. *Frontiers in Molecular Biosciences*, 8, 729513.

991 Honorato, R. V., Trellet, M. E., Jiménez-García, B., Schaarschmidt, J. J., Giulini, M., Reys, V.,
992 Koukos, P. I., Rodrigues, J. P. G. L. M., Karaca, E., van Zundert, G. C. P., Roel-Touris, J., van
993 Noort, C. W., Jandova, Z., Melquiond, A. S. J., and Bonvin, A. M. (2024). The HADDOCK2. 4
994 web server for integrative modeling of biomolecular complexes. *Nature Protocols*, 1-23.

995 Hopper, N. A., Harwood, A. J., Bouzid, S., Veron, M., and Williams, J. G. (1993). Activation of
996 the prespore and spore cell pathway of *Dictyostelium* differentiation by cAMP-dependent protein
997 kinase and evidence for its upstream regulation by ammonia. *The EMBO Journal*, 12(6), 2459-
998 2466.

999 Huber, R. J., Williams, R. S., and Müller-Taubenberger, A. (2022). *Dictyostelium*: A Tractable
1000 Cell and Developmental Model in Biomedical Research. *Frontiers in Cell and Developmental*
1001 *Biology*, 10, 909619.

1002 Iijima, R., Kunieda, T., Yamaguchi, S., Kamigaki, H., Fujii-Taira, I., Sekimizu, K., Kubo, T.,
1003 Natori, S., Homma, K. J. (2008). The extracellular adenosine deaminase growth factor,
1004 ADGF/CECR1, plays a role in *Xenopus* embryogenesis via the adenosine/P1 receptor. *J Biol*
1005 *Chem*. 283(4):2255–2264.

1006 Inouye, K. (1989). Control of cell type proportions by a secreted factor in *Dictyostelium*
1007 *discoideum*. *Development*, 107(3), 605-609.

1008 Jaiswal, P., Soldati, T., Thewes, S., and Baskar, R. (2012). Regulation of aggregate size and
1009 pattern by adenosine and caffeine in cellular slime molds. *BMC Developmental Biology*, *12*, 1-19.

1010 Jang, W., and Gomer, R. H. (2011). Initial cell type choice in *Dictyostelium*. Eukaryotic Cell,
1011 10(2), 150-155.

1012 Jumper, J et. al., (2021). Highly accurate protein structure prediction with
1013 alphafold. *Nature*, 596(7873), 583-589.

1014 Kay, R. R., Tilly, R., and Garrod, D. (1978). Requirement for cell differentiation in
1015 *Dictyostelium discoideum*. *Nature*, 271(5640), 58-60.

1016 Kellerman, K. A., and McNally, J. G. (1999). Mound-Cell Movement and Morphogenesis in
1017 *Dictyostelium*. *Developmental Biology*, *208*(2), 416-429.

1018 Kessin, R. H. (2001). *Dictyostelium*: evolution, cell biology, and the development of
1019 multicellularity (Vol. 38). Cambridge University Press.

1020 Khachatrian, L., Klein, C., and Howlett, A. (1987). Regulation of *Dictyostelium discoideum*
1021 adenylate cyclase by manganese and adenosine analogs. *Biochimica et Biophysica Acta (BBA)-*
1022 *Molecular Cell Research*, 927(2), 235-246.

1023 Kirsten, J. H., Xiong, Y., Dunbar, A. J., Rai, M., and Singleton, C. K. (2005). Ammonium
1024 transporter C of *Dictyostelium discoideum* is required for correct prestalk gene expression and
1025 for regulating the choice between slug migration and culmination. *Developmental*
1026 *Biology*, 287(1), 146-156.

1027 Koehl, P. (2001). Protein structure similarities. *Current Opinion in Structural Biology*, 11(3),
1028 348-353.

1029 Konijn, T. M., Van De Meene, J. G., Bonner, J. T., and Barkley, D. S. (1967). The acrasin
1030 activity of adenosine-3', 5'-cyclic phosphate. *Proceedings of the National Academy of Sciences*
1031 *(USA)*, 58(3), 1152-1154.

1032 Kosugi, T., and Inouye, K. (1989). Negative chemotaxis to ammonia and other weak bases by
1033 migrating slugs of the cellular slime moulds. *Microbiology*, 135(6), 1589-1598.

1034 Kumar, S., Stecher, G., Li, M., Knyaz, C., and Tamura, K. (2018). MEGA X: molecular
1035 evolutionary genetics analysis across computing platforms. *Molecular Biology and*
1036 *Evolution*, 35(6), 1547.

1037 Lam, T., Pickering, G., Geltosky, J., and Siu, C. H. (1981). Differential cell cohesiveness
1038 expressed by prespore and prestalk cells of *Dictyostelium discoideum*. *Differentiation*, *20*(1-3),
1039 22-28.

1040 Lane, M., and Gardner, D. K. (2003). Ammonium induces aberrant blastocyst differentiation,
1041 metabolism, pH regulation, gene expression and subsequently alters fetal development in the
1042 mouse. *Biology of Reproduction*, 69(4), 1109-1117.

1043 Letunic, I., and Bork, P. (2018). 20 years of the SMART protein domain annotation
1044 resource. *Nucleic Acids Research*, 46(D1), D493-D496.

1045 Li, S., and Aksoy, S. (2000). A family of genes with growth factor and adenosine deaminase
1046 similarity are preferentially expressed in the salivary glands of *Glossina m. morsitans*. *Gene*,
1047 252(1-2), 83-93.

1048 Lipkowski, J., and Galus, Z. (1973). Electrode kinetics in mixed solvents Investigations of the
1049 kinetics and equilibrium properties of manganese (II)—ammonia complexes in water and mixed
1050 solvents of n-propanol, isopropanol, t-butanol and water. *Journal of Electroanalytical Chemistry*
1051 *and Interfacial Electrochemistry*, 48(3), 337-352.

1052 Liu, Y., Zhang, X., Wang, W., Liu, T., Ren, J., Chen, S., Lu, T., Yuan, X., Mo, F., Yang, J, Wei,
1053 Y., and Wei, X. (2022). Ammonia promotes the proliferation of bone marrow-derived
1054 mesenchymal stem cells by regulating the Akt/mTOR/S6k pathway. *Bone Research*, 10(1), 57.

1055 Lonski, J. (1976). The effect of ammonia on fruiting body size and microcyst formation in the
1056 cellular slime molds. *Developmental Biology*, 51(1), 158-165.

1057 Loomis, W. F., Klein, C., and Bracket, P. (1979). The effect of divalent cations on aggregation of
1058 *Dictyostelium discoideum*. *Differentiation*, 12(1-3), 83-89.

1059 Lu, J., Li, Y., Zhang, C., Yang, X., and Qiang, J. W. (2020). Interaction of manganese and
1060 ammonia in the brain of hepatic encephalopathy rats. *Hepatitis Monthly*, 20(8).

1061 Mahadeo, D. C., and Parent, C. A. (2006). Signal relay during the life cycle of
1062 *Dictyostelium*. *Current topics in Developmental Biology*, *73*, 115-140.

1063 Maier, S. A., Galellis, J. R., and McDermid, H. E. (2005). Phylogenetic analysis reveals a novel
1064 protein family closely related to adenosine deaminase. *Journal of Molecular Evolution*, 61, 776-
1065 794.

1066 Mann, S. K., and Firtel, R. A. (1993). cAMP-dependent protein kinase differentially regulates
1067 prestalk and prespore differentiation during *Dictyostelium* development. *Development*, *119*(1),
1068 135-146.

1069 Marone, G., Plaut, M., and Lichtenstein, L. M. (1980). The role of adenosine in the control of
1070 immune function. *Ricerca in clinica e in laboratorio*., 10(2), 303-312.

1071 Martín-González, J., Montero-Bullón, J. F., and Lacal, J. (2021). *Dictyostelium discoideum* as a
1072 non-mammalian biomedical model. *Microbial Biotechnology*, 14(1), 111-125.

1073 Meinhardt, H. (1983). A model for the prestalk/prespore patterning in the slug of the slime
1074 mold *Dictyostelium discoideum*. *Differentiation*, 24(1-3), 191-202.

1075 Mizushima, N., Levine, B., Cuervo, A. M., and Klionsky, D. J. (2008). Autophagy fights disease
1076 through cellular self-digestion. *Nature*, 451(7182), 1069-1075.

1077 Moreno, E., Canet, J., Gracia, E., Lluís, C., Mallol, J., Canela, E. I., Cortés. A. and Casadó, V.
1078 (2018). Molecular Evidence of Adenosine Deaminase Linking Adenosine A2A Receptor and
1079 CD26 Proteins. *Frontiers in Pharmacology*, 9, 106.

1080 Müller-Taubenberger, A., Kortholt, A., and Eichinger, L. (2013). Simple system–substantial
1081 share: the use of *Dictyostelium* in cell biology and molecular medicine. *European Journal of Cell*
1082 *Biology*, 92(2), 45-53.

1083 Nadin, B. M., Mah, C. S., Scharff, J. R., and Ratner, D. I. (2000). The regulative capacity of
1084 prespore amoebae as demonstrated by fluorescence-activated cell sorting and green fluorescent
1085 protein. *Developmental Biology*, 217(1), 173-178.

1086 Nassir, N., Hyde, G. J., and Baskar, R. (2019). A telomerase with novel non-canonical roles:
1087 TERT controls cellular aggregation and tissue size in *Dictyostelium*. *PLoS Genetics*, *15*(6),
1088 e1008188.

1089 Neave, N., Sobolewski, A., and Weeks, G. (1983). The effect of ammonia on stalk cell formation
1090 in submerged monolayers of *Dictyostelium discoideum*. *Cell Differentiation*, 13(4), 301-307.

1091 Needham, J. (1926). The energy-sources in ontogenesis: III. The ammonia content of the
1092 developing avian egg and the theory of recapitulation. *Journal of Experimental Biology*, 4(2),
1093 145-154.

1094 Newell, P. C., Telser, A., and Sussman, M. (1969). Alternative developmental pathways
1095 determined by environmental conditions in the cellular slime mold *Dictyostelium*
1096 *discoideum*. *Journal of Bacteriology*, 100(2), 763-768.

1097 Newell, P. C. (1982). Cell surface binding of adenosine to *Dictyostelium* and inhibition of
1098 pulsatile signaling. *FEMS Microbiology Letters*, 13(4), 417-421.

1099 Notarangelo, L. D. (2016). T cell immunodeficiencies. *Paediatric Allergy, E-Book: Principles*
1100 *and Practice*, 80-89.

1101 Otto, G. P., Wu, M. Y., Kazgan, N., Anderson, O. R., and Kessin, R. H. (2003). Macroautophagy
1102 is required for multicellular development of the social amoeba *Dictyostelium discoideum*.
1103 *Journal of Biological Chemistry*, 278(20), 17636-17645.

1104 Otto, G. P., Wu, M. Y., Clarke, M., Lu, H., Anderson, O. R., Hilbi, H., Shuman, H, A and Kessin,
1105 R. H. (2004). Macroautophagy is dispensable for intracellular replication of *Legionella*
1106 *pneumophila* in *Dictyostelium discoideum*. *Molecular Microbiology*, *51*(1), 63-72.

1107 Oyama, M., and Blumberg, D. D. (1986). Cyclic AMP and $NH_3/NH^{+}{}_4$ both regulate cell-type-
1108 specific mRNA accumulation in the cellular slime mold, *Dictyostelium*
1109 *discoideum*. *Developmental Biology*, 117(2), 557-566.

1110 Palková, Z., Janderová, B., Gabriel, J., Zikánová, B., Pospíŝek, M., and Forstová, J. (1997).
1111 Ammonia mediates communication between yeast colonies. *Nature*, 390(6659), 532-536.

1112 Palková, Z., and Forstová, J. (2000). Yeast colonies synchronise their growth and development.
1113 *Journal of Cell Science*, 113(11), 1923-1928.

1114 Palsson, E., and Cox, E. C. (1996). Origin and evolution of circular waves and spirals in
1115 *Dictyostelium discoideum* territories. *Proceedings of the National Academy of Sciences (USA)*,
1116 93(3), 1151-1155.

1117 Pijuan-Sala, B., Griffiths, J. A., Guibentif, C., Hiscock, T. W., Jawaid, W., Calero-Nieto, F. J.,
1118 Mulas, C., Ibarra-Soria, X., Tyser, R. C. V, Ho, D. L. L., Reik, W., Srinivas, S., Simons, D. B.,
1119 Nichols, J., Marioni, J.C., and Göttgens, B. (2019). A single-cell molecular map of mouse
1120 gastrulation and early organogenesis. *Nature*, 566(7745), 490-495.

1121 Poole, B., and Ohkuma, S. (1981). Effect of weak bases on the intralysosomal pH in mouse
1122 peritoneal macrophages. *The Journal of Cell Biology*, 90(3), 665-669.

1123 Raper, K. B. (1940). Pseudoplasmodium formation and organization in *Dictyostelium*
1124 discoideum. *Journal of the Elisha Mitchell Scientific Society*, 56(2), 241-282.

1125 Riazi, A. M., Arsdell, G. V., and Buchwald, M. (2005). Transgenic expression of CECR1
1126 adenosine deaminase in mice results in abnormal development of heart and kidney. *Transgenic*
1127 *Research*, 14, 333-336.

1128 Ribeiro, J. A., and Sebastiao, A. M. (2010). Caffeine and adenosine. *Journal of Alzheimer's*
1129 *Disease*, 20(s1), S3-S15.

1130 Riley, B. B., and Barclay, S. L. (1990). Ammonia promotes accumulation of intracellular cAMP
1131 in differentiating amoebae of *Dictyostelium discoideum*. *Development*, 109(3), 715-722.

1132 Rivera-Mancía, S., Ríos, C., and Montes, S. (2012). Manganese and ammonia interactions in the
1133 brain of cirrhotic rats: effects on brain ammonia metabolism. *Neurochemical Research*, 37,
1134 1074-1084.

1135 Roisin-Bouffay, C., Jang, W., Caprette, D. R., and Gomer, R. H. (2000). A precise group size in
1136 *Dictyostelium* is generated by a cell-counting factor modulating cell–cell adhesion. *Molecular*
1137 *Cell*, 6(4), 953-959.

1138 Rubin, J., and Robertson, A. (1975). The tip of the *Dictyostelium discoideum* pseudoplasmodium
1139 as an organizer. *Development*, 33(1), 227-241.

1140 Saitou, N., and Nei, M. (1987). The neighbor-joining method: a new method for reconstructing
1141 phylogenetic trees. *Molecular Biology and Evolution*, 4(4), 406-425.

1142 Sawai, S., Hirano, T., Maeda, Y., and Sawada, Y. (2002). Rapid patterning and zonal
1143 differentiation in a two-dimensional *Dictyostelium* cell mass: the role of pH and ammonia.
1144 *Journal of Experimental Biology*, 205(17), 2583-2590.

1145 Saxe, C. 3., Ginsburg, G. T., Louis, J. M., Johnson, R., Devreotes, P. N., and Kimmel, A. R.
1146 (1993). CAR2, a prestalk cAMP receptor required for normal tip formation and late development
1147 of *Dictyostelium discoideum*. *Genes and Development*, 7(2), 262-272.

1148 Schaap, P., Brandt, R., and van Es, S. (1995). Regulation of *Dictyostelium* adenylylcyclases by
1149 morphogen-induced modulation of cytosolic pH or Ca^{2+} levels. *Developmental Biology*, 168(1),
1150 179-188.

1151 Schaap, P., and Wang, M. (1986). Interactions between adenosine and oscillatory cAMP
1152 signaling regulate size and pattern in *Dictyostelium*. *Cell*, 45(1), 137-144.

1153 Schindler, J., and Sussman, M. (1977). Ammonia determines the choice of morphogenetic
1154 pathways in *Dictyostelium discoideum*. *Journal of Molecular Biology*, 116(1), 161-169.

1155 Schindler, J., and Sussman, M. (1979). Inhibition by ammonia of intracellular cAMP
1156 accumulation in *Dictyostelium discoideum*: its significance for the regulation of
1157 morphogenesis. *Developmental Genetics*, 1(1), 13-20.

1158 Schmittgen, T. D., and Livak, K. J. (2008). Analyzing real-time PCR data by the comparative CT
1159 method. *Nature protocols*, 3(6), 1101-1108.

1160 Schulz-Bohm, K., Martín-Sánchez, L., and Garbeva, P. (2017). Microbial volatiles: small
1161 molecules with an important role in intra and inter-kingdom interactions. *Frontiers in*
1162 *Microbiology*, 8, 289291.

1163 Schultz, R. D., and Gumienny, T. L. (2012). Visualization of *Caenorhabditis elegans* cuticular
1164 structures using the lipophilic vital dye DiI. *Journal of Visualized Experiments*, (59), e3362.

1165 Siegert, F., and Weijer, C. (1989). Digital image processing of optical density wave propagation
1166 in *Dictyostelium discoideum* and analysis of the effects of caffeine and ammonia. *Journal of Cell*
1167 *Science*, 93(2), 325-335.

1168 Siegert, F., and Weijer, C. J. (1995). Spiral and concentric waves organize multicellular
1169 *Dictyostelium* mounds. *Current Biology*, 5(8), 937-943.

1170 Singer, G., Araki, T., and Weijer, C. J. (2019). Oscillatory cAMP cell-cell signaling persists
1171 during multicellular *Dictyostelium* development. *Communications Biology*, *2*(1), 139.

1172 Singh, S. P., and Insall, R. H. (2022). Under-Agarose Chemotaxis Chemotaxis and Migration
1173 Assays for *Dictyostelium*. In *Cell Polarity Signaling: Methods and Protocols* (pp. 467-482). New
1174 York, NY: Springer US.

1175 Singleton, C. K., Zinda, M. J., Mykytka, B., and Yang, P. (1998). The histidine kinase dhkC
1176 regulates the choice between migrating slugs and terminal differentiation in *Dictyostelium*
1177 *discoideum*. *Developmental Biology*, 203(2), 345-357.

1178 Singleton, C. K., Kirsten, J. H., and Dinsmore, C. J. (2006). Function of ammonium transporter
1179 A in the initiation of culmination of development in *Dictyostelium discoideum*. *Eukaryotic*
1180 *Cell*, 5(7), 991-996.

1181 Singleton, C. K., and Xiong, Y. (2013). Loss of the histidine kinase DhkD results in mobile
1182 mounds during development of *Dictyostelium discoideum*. *Plos One*, 8(9), e75618.

1183 Siu, C. H., Lam, T. Y., and Choi, A. H. (1985). Inhibition of cell-cell binding at the aggregation
1184 stage of *Dictyostelium discoideum* development by monoclonal antibodies directed against an
1185 80,000-dalton surface glycoprotein. *Journal of Biological Chemistry*, 260(29), 16030-16036.

1186 Steer, M. L. (1975). Adenyl cyclase. *Annals of Surgery*, 182(5), 603.

1187 Stege, J. T., Laub, M. T., and Loomis, W. F. (1999). Tip genes act in parallel pathways of early
1188 *Dictyostelium* development. *Developmental Genetics*, 25(1), 64-77.

1189 Stein, L. Y., Campbell, M. A., and Klotz, M. G. (2013). Energy-mediated vs. ammonium-
1190 regulated gene expression in the obligate ammonia-oxidizing bacterium, *Nitrosococcus oceani*.
1191 *Frontiers in Microbiology*, 4, 277.

1192 Sternfeld, J., and David, C. N. (1979). Ammonia plus another factor are necessary for
1193 differentiation in submerged clumps of *Dictyostelium*. *Journal of Cell Science*, 38(1), 181-191.

1194 Sternfeld, J., and David, C. N. (1982). Fate and regulation of anterior-like cells in *Dictyostelium*
1195 slugs. *Developmental Biology*, 93(1), 111-118.

1196 Tanaka, T., Kameoka, J., Yaron, A., Schlossman, S. F., and Morimoto, C. (1993). The
1197 costimulatory activity of the CD26 antigen requires dipeptidyl peptidase IV enzymatic activity.
1198 *Proceedings of the National Academy of Sciences (USA)*, 90(10), 4586-4590.

1199 Taya, Y., Tanaka, Y., and Nishimura, S. (1978). 5′-AMP is a direct precursor of cytokinin in
1200 *Dictyostelium discoideum*. *Nature*, 271(5645), 545-547.

1201 Thadani, V., Pan, P., and Bonner, J. T. (1977). Complementary effects of ammonia and cAMP
1202 on aggregation territory size in the cellular slime mold *Dictyostelium mucoroides*. *Experimental*
1203 *Cell Research*, 108(1), 75-78.

1204 Theibert, A., and Devreotes, P. N. (1984). Adenosine and its derivatives inhibit the cAMP
1205 signaling response in *Dictyostelium discoideum*. *Developmental Biology*, 106(1), 166-173.

1206 Thomason, P., Traynor, D., and Kay, R. (1999). Taking the plunge: terminal differentiation in
1207 *Dictyostelium*. *Trends in Genetics*, 15(1), 15-19.

1208 Torija, P., Vicente, J. J., Rodrigues, T. B., Robles, A., Cerdán, S., Sastre, L., Martínez, P., and
1209 Escalante, R. (2006). Functional genomics in *Dictyostelium*: MidA, a new conserved protein, is
1210 required for mitochondrial function and development. *Journal of Cell Science*, 119(6), 1154-
1211 1164.

1212 Traynor, D., Kessin, R. H., and Williams, J. G. (1992). Chemotactic sorting to cAMP in the
1213 multicellular stages of *Dictyostelium* development. *Proceedings of the National Academy of*
1214 *Sciences (USA)*, 89(17), 8303-8307.

1215 Tung, S. M., Ünal, C., Ley, A., Peña, C., Tunggal, B., Noegel, A. A., Krut, O., Steinert, M., and
1216 Eichinger, L. (2010). Loss of *Dictyostelium* ATG9 results in a pleiotropic phenotype affecting

1217 growth, development, phagocytosis and clearance and replication of *Legionella pneumophila*.
1218 *Cellular Microbiology*, 12(6), 765-780.

1219 Tyser, R. C., Mahammadov, E., Nakanoh, S., Vallier, L., Scialdone, A., and Srinivas, S. (2021).
1220 Single-cell transcriptomic characterization of a gastrulating human embryo. *Nature*, 600(7888),
1221 285-289.

1222 Tzertzinis, G., Ganatra, M. B., Ruse, C., Taron, C. H., Causey, B., Wang, L., and Schildkraut, I.
1223 (2023). The AMP deaminase of the mollusk *Helix pomatia* is an unexpected member of the
1224 adenosine deaminase-related growth factor (ADGF) family. *PloS One*, 18(7), e0286435.

1225 Ubeidat, M., Eristi, C. M., and Rutherford, C. L. (2002). Expression pattern of 5′-nucleotidase in
1226 *Dictyostelium*. *Mechanisms of Development*, *110*(1-2), 237-239.

1227 Van Duijn, B., and Inouye, K. (1991). Regulation of movement speed by intracellular pH during
1228 *Dictyostelium discoideum* chemotaxis. *Proceedings of the National Academy of Sciences (USA)*,
1229 88(11), 4951-4955.

1230 Van Haastert, P. J. (1983). Binding of cAMP and adenosine derivatives to *Dictyostelium*
1231 *discoideum* cells. Relationships of binding, chemotactic, and antagonistic activities. *Journal of*
1232 *Biological Chemistry*, 258(16), 9643-9648.

1233 Wakamiya, M., Blackburn, M. R., Jurecic, R., McArthur, M. J., Geske, R. S., Cartwright Jr, J.,
1234 and Kellems, R. E. (1995). Disruption of the adenosine deaminase gene causes hepatocellular
1235 impairment and perinatal lethality in mice. *Proceedings of the National Academy of Sciences*
1236 *(USA)*, 92(9), 3673-3677.

1237 Walsh, J., and Wright, B. E. (1978). Kinetics of net RNA degradation during development in
1238 *Dictyostelium discoideum*. *Microbiology*, 108(1), 57-62.

1239 Wang, B., and Kuspa, A. (2002). CulB, a putative ubiquitin ligase subunit, regulates prestalk cell
1240 differentiation and morphogenesis in *Dictyostelium* spp. *Eukaryotic Cell*, 1(1), 126-136.

1241 Wang, M., and Schaap, P. (1985). Correlations between tip dominance, prestalk/prespore pattern,
1242 and cAMP-relay efficiency in slugs of *Dictyostelium discoideum*. *Differentiation*, 30(1), 7-14.

1243 Wang, M., and Schaap, P. (1989). Ammonia depletion and DIF trigger stalk cell differentiation
1244 in intact *Dictyostelium discoideum* slugs. *Development*, 105(3), 569-574.

1245 Weeks, G., and Weijer, C. J. (1994). The *Dictyostelium* cell cycle and its relationship to
1246 differentiation. *FEMS Microbiology Letters*, 124(2), 123-130.

1247 Weijer, C. J. (2009). Collective cell migration in development. *Journal of Cell Science*, 122(18),
1248 3215-3223.

1249 Weijer, C. J., and Durston, A. J. (1985). Influence of cyclic AMP and hydrolysis products on cell
1250 type regulation in *Dictyostelium discoideum*. *Development*, 86(1), 19-37.

1251 White, G. J., and Sussman, M. (1961). Metabolism of major cell components during slime mold
1252 morphogenesis. *Biochimica et biophysica acta*, 53(2), 285-293.

1253 Wiechetek, M., Breves, G., and Höller, H. (1979). The effect of ammonium ion concentration on
1254 the activity of adenylate cyclase in various rat tissues in vitro. *Quarterly Journal of Experimental*
1255 *Physiology and Cognate Medical Sciences: Translation and Integration*, 64(3), 169-174.

1256 Williams, G. B., Elder, E. M., and Sussman, M. (1984). Modulation of the cAMP relay in
1257 *Dictyostelium discoideum* by ammonia and other metabolites: possible morphogenetic
1258 consequences. *Developmental Biology*, 105(2), 377-388.

1259 Williams, J. G. (1988). The role of diffusible molecules in regulating the cellular differentiation
1260 of *Dictyostelium discoideum*. *Development*, 103(1), 1-16.

1261 Williams, J. G. (2006). Transcriptional regulation of *Dictyostelium* pattern formation. *EMBO*
1262 *Reports*, 7(7), 694-698.

1263 Williams, J. G., Duffy, K. T., Lane, D. P., McRobbie, S. J., Harwood, A. J., Traynor, D., Kay, R.
1264 R. and Jermyn, K. A. (1989). Origins of the prestalk-prespore pattern in *Dictyostelium*
1265 development. *Cell*. 59(6), 1157–1163.

1266 Woznica, D., and Knecht, D. A. (2006). Under-agarose chemotaxis of *Dictyostelium discoideum*.
1267 In *Dictyostelium discoideum* protocols (pp. 311-325). Totowa, NJ: Humana Press.

1268 Xu, J., Wang, X., Chen, J., Chen, S., and Li, Z., Liu, H., Bai, Y and Zhi, F. (2020). Embryonic
1269 stem cell-derived mesenchymal stem cells promote colon epithelial integrity and regeneration by
1270 elevating circulating IGF-1 in colitis mice. *Theranostics,* 10(26), 12204.

1271 Yamada, T. (1950). Dorsalization of the ventral marginal zone of the *Triturus* gastrula. I.
1272 Ammonia-treatment of the medio-ventral marginal zone. *The Biological bulletin*, 98(2), 98-121.

1273 Yeung, S. M. H., Shoshani, I., Stübner, D., and Johnson, R. A. (1989). Ammonium ions enhance
1274 proteolytic activation of adenylate cyclase and decrease its sensitivity to inhibition by "P"-site
1275 agonists. *Archives of Biochemistry and Biophysics*, 271(2), 332-345.

1276 Yoshino, R., Morio, T., Yamada, Y., Kuwayama, H., Sameshima, M., Tanaka, Y., Sesaki, H.,
1277 and Iijima, M. (2007). Regulation of ammonia homeostasis by the ammonium transporter AmtA
1278 in *Dictyostelium discoideum*. *Eukaryotic Cell*, 6(12), 2419-2428.

1279 Zavialov, A. V., Yu, X., Spillmann, D., Lauvau, G., and Zavialov, A. V. (2010). Structural basis
1280 for the growth factor activity of human adenosine deaminase ADA2. *Journal of Biological*
1281 *Chemistry*, 285(16), 12367-12377.

1282 Zhou, Q et al. (2014). Early-onset stroke and vasculopathy associated with mutations in
1283 ADA2. *New England Journal of Medicine*, 370(10), 911-920.

1284 Zurovec, M., Dolezal, T., Gazi, M., Pavlova, E., and Bryant, P. J. (2002). Adenosine deaminase-
1285 related growth factors stimulate cell proliferation in *Drosophila* by depleting extracellular
1286 adenosine. *Proceedings of the National Academy of Sciences (USA)* 99(7), 4403-4408.

Figure 1

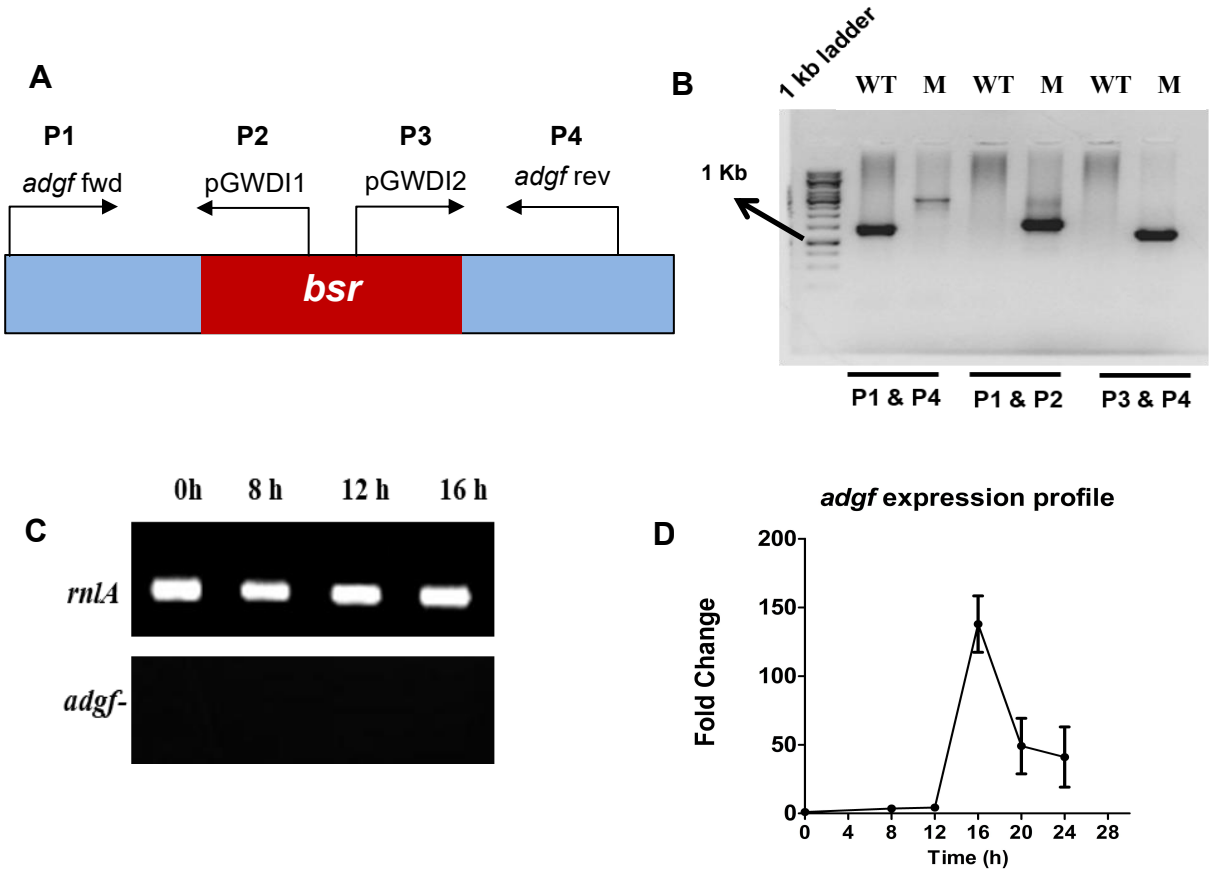

Figure 1. *adgf* mutant validation

A) Schematic representation of *adgf* locus showing the relative positions of the primers (P1–P4) and the blasticidin resistance cassette (*bsr*). Primer P1 (*adgf* fwd) is at the start codon of *adgf*, and primer P4 (*adgf* rev) is 264 bp upstream of the stop codon, flanking the insertion site. Primers P2 (pGWD2) and P3 (pGWD1) are located within the *bsr* cassette. *bsr* insertion is in exon 2 of *adgf*. **B)** PCR analyses using P1 and P4 primers. A 1.4 kb shift in the *adgf* mutant. PCR using P1 and P2 primers showed an amplicon from the mutant (M) and not from the wild type (WT). PCR using P3 and P4 primers showed an amplicon with the *adgf* mutant while WT did not show any amplicon. **C)** Semi-quantitative RT-PCR of the internal control, *rnlA* and *adgf*$^{-}$. *adgf* expression during development in *Dictyostelium*. **D)** Total RNA was isolated from *Dictyostelium* during vegetative growth and development using TRIzol method. To quantify *adgf* expression, qRT-PCR was carried out with *rnlA* as a control and the fold change was calculated accordingly. Time points are shown in hours (bottom). Error bars represent the mean and SEM (n = 3).

Figure 2

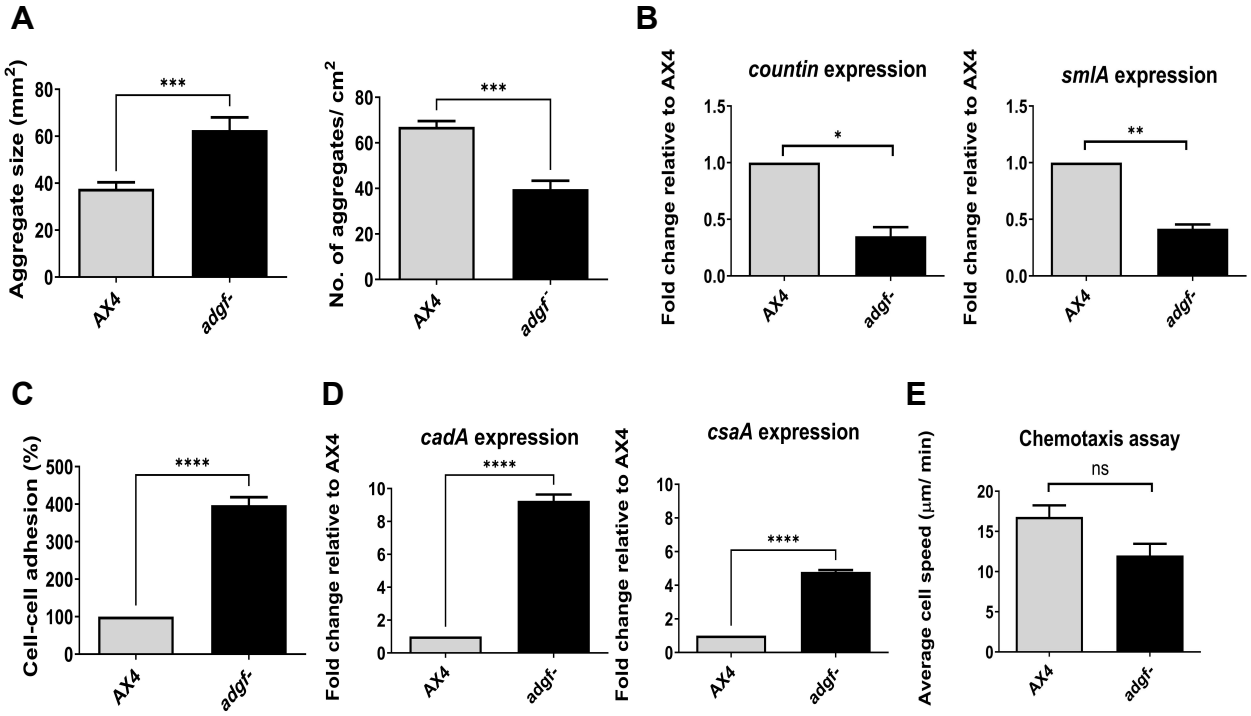
A
Aggregate size (mm²)
***
AX4
adgf-
No. of aggregates/ cm²
***
AX4
adgf-
B
countin expression
Fold change relative to AX4
*
AX4
adgf-
smlA expression
Fold change relative to AX4
**
AX4
adgf-
C
Cell-cell adhesion (%)
****
AX4
adgf-
D
cadA expression
Fold change relative to AX4
****
AX4
adgf-
csaA expression
Fold change relative to AX4
****
AX4
adgf-
E
Chemotaxis assay
Average cell speed (µm/ min)
ns
AX4
adgf-

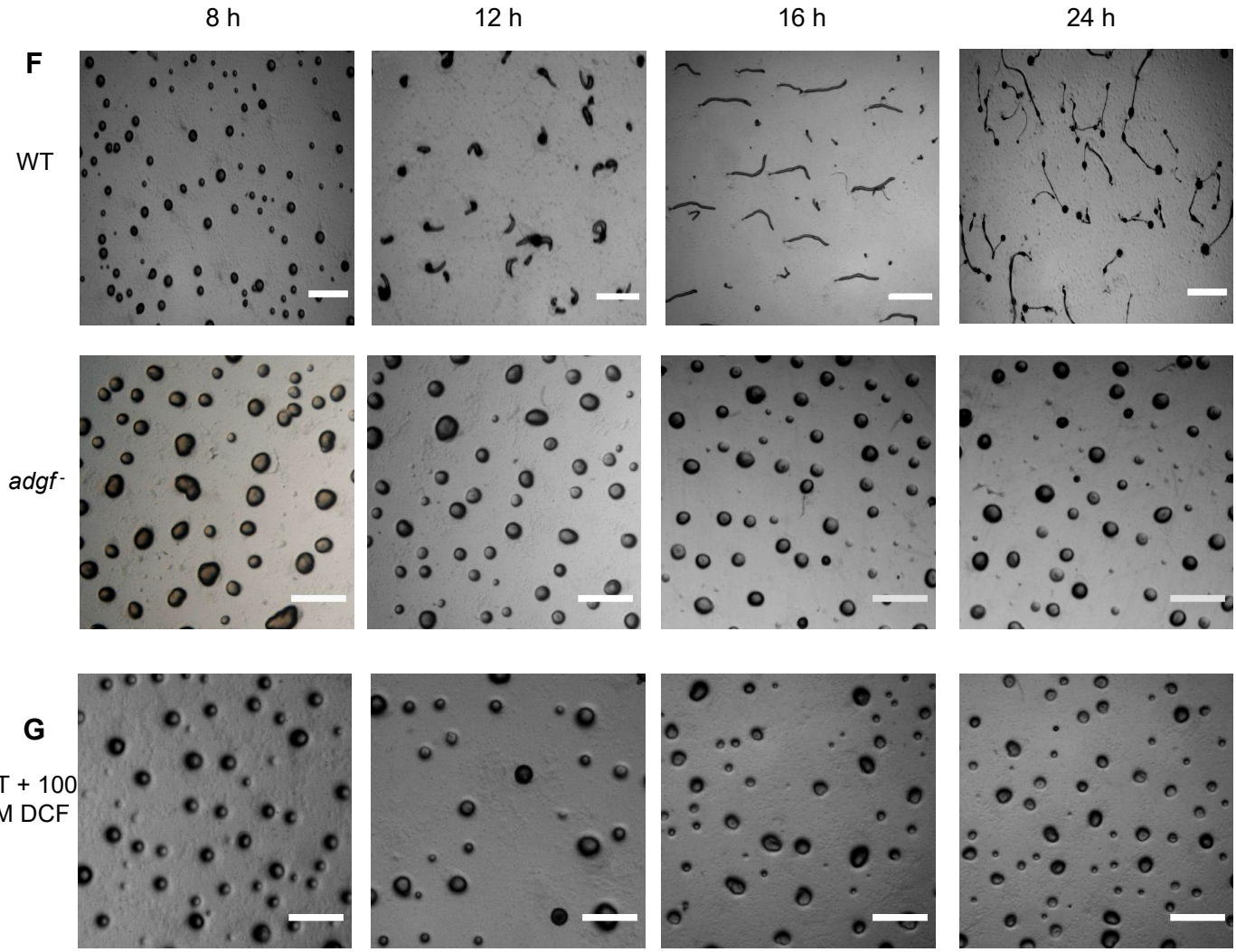
8 h
12 h
16 h
24 h
F
WT
adgf-
G
WT + 100 nM DCF

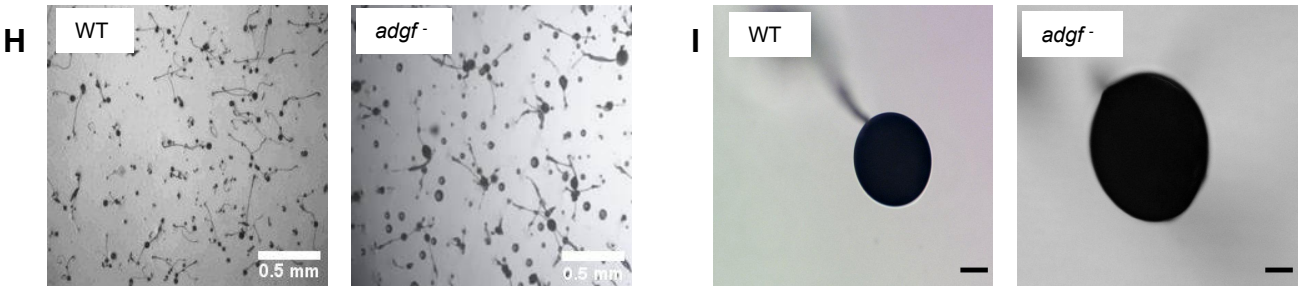

Figure 2. Aggregates formed by *adgf* mutants were larger in size

A) The graph shows the mound size and the number of aggregates formed by WT and *adgf* $^{-}$. The values represent mean ± S.E; n=3. **B)** Expression levels of the genes, countin (*ctn*) and small aggregates (*smlA*) during aggregation in *adgf* $^{-}$ compared to WT. *rnlA* was used as the internal control. **C)** WT and *adgf* $^{-}$ cells were developed on KK2 agar, and after 16 h, the multicellular mounds/slugs were dissociated by vigorous vortexing in KK2 buffer. Individual cells were counted using a hemocytometer and resuspended in a phosphate buffer. Non-adherent single cells were counted 45 min after incubation. The percent cell-cell adhesion was plotted by normalizing the values to the non-adherent WT count to 100%. Error bars represent the mean ± SEM (n=3). **D)** qRT-PCR analysis of cadherin (*cadA*) and contact site (*csA*) during aggregation. The fold-change in RNA transcript levels is relative to WT at the indicated time points. (n=3). ns = not significant. Significance level is indicated as *p< 0.05, **p< 0.01, ***p< 0.001, ****p< 0.0001. (Student's t-test). **E)** Under agarose chemotaxis assay. The average cell speed in response to 10 µM cAMP was recorded. The graph represents the mean ± SEM (n=3). **Developmental phenotype of *adgf* $^{-}$. F)** WT and *adgf* $^{-}$ cells were washed, plated on 1% KK2 agar plates at a density of $5x10^5$ cells/cm^2, incubated in a dark, moist chamber and images were taken at different time intervals. **G)** WT cells treated with 100 nM of DCF mimicked the mound arrest phenotype of the mutant. The time points are indicated in hours at the top of the figure. Scale bar: 2 mm; (n=3). **H)** WT and *adgf* $^{-}$ cells after 36 h of development. Scale bar: 0.5 mm; (n=3). **I)** Fruiting bodies of WT and *adgf* $^{-}$. Scale bar: 2 mm; (n=3).

Figure 3

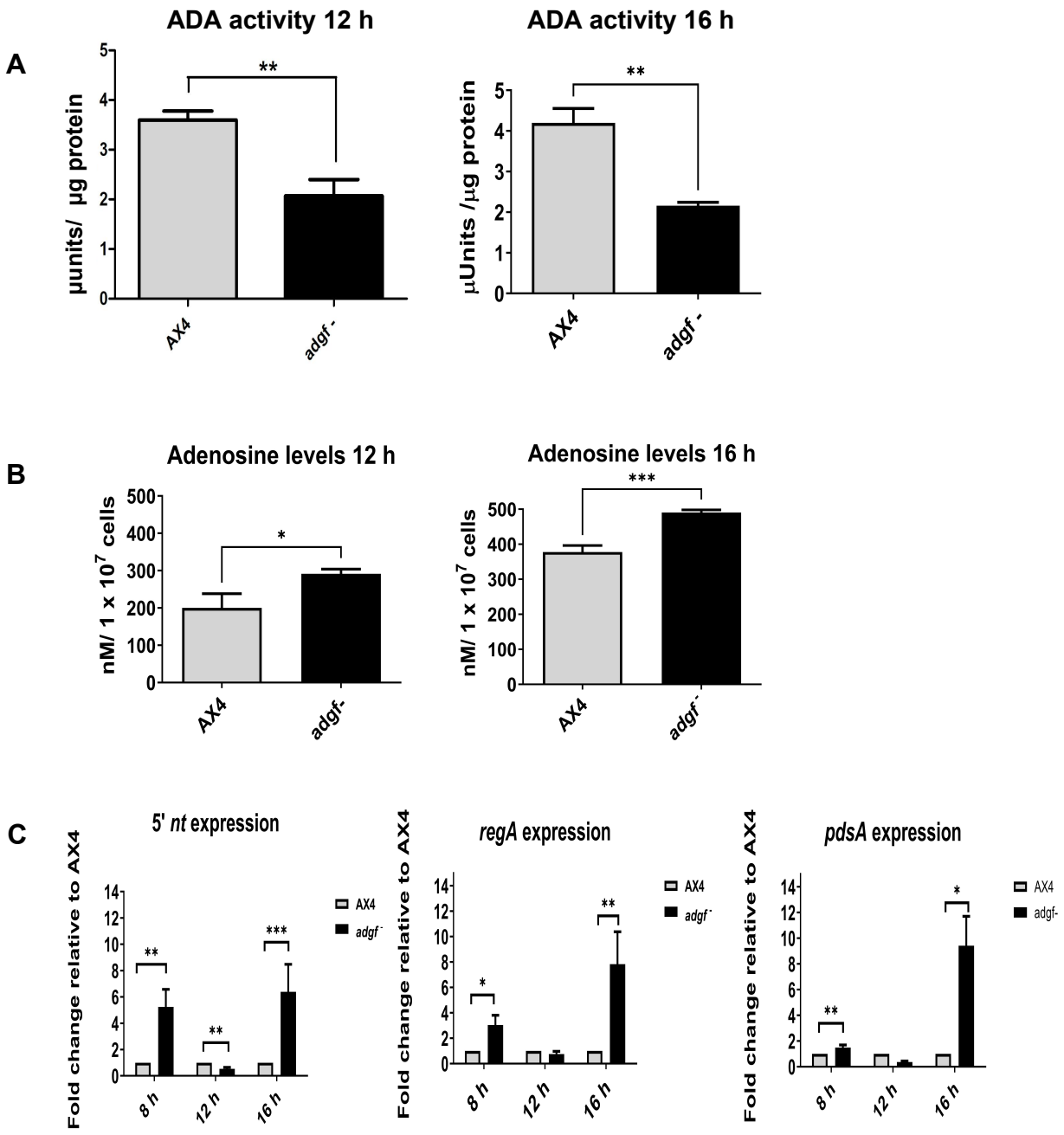

Figure 3. *adgf* mounds have reduced ADA activity and high adenosine levels.

A) ADA activity in WT and *adgf* $^{-}$ harvested at 12 h and 16 h. The enzymatic assay for ADA was performed in *adgf* $^{-}$ with the corresponding WT control. Error bars represent the mean and SEM (n=3). Significance level is indicated as **p< 0.01. **B)** Quantification of adenosine levels in WT and *adgf* mutants at 12 h and 16 h. Level of significance is indicated as *p< 0.05, **p< 0.01, ***p< 0.001; (n=3). **C)** Expression profile of 5' nucleotidase (*5'nt*) and phosphodiesterases (*regA*, *pdsA*) involved in cAMP-to-adenosine conversion. The fold-change in RNA transcript levels is relative to WT at the indicated time points. *rnlA* was used as an internal control. Error bars represent the mean and SEM (n=3).

Figure 4

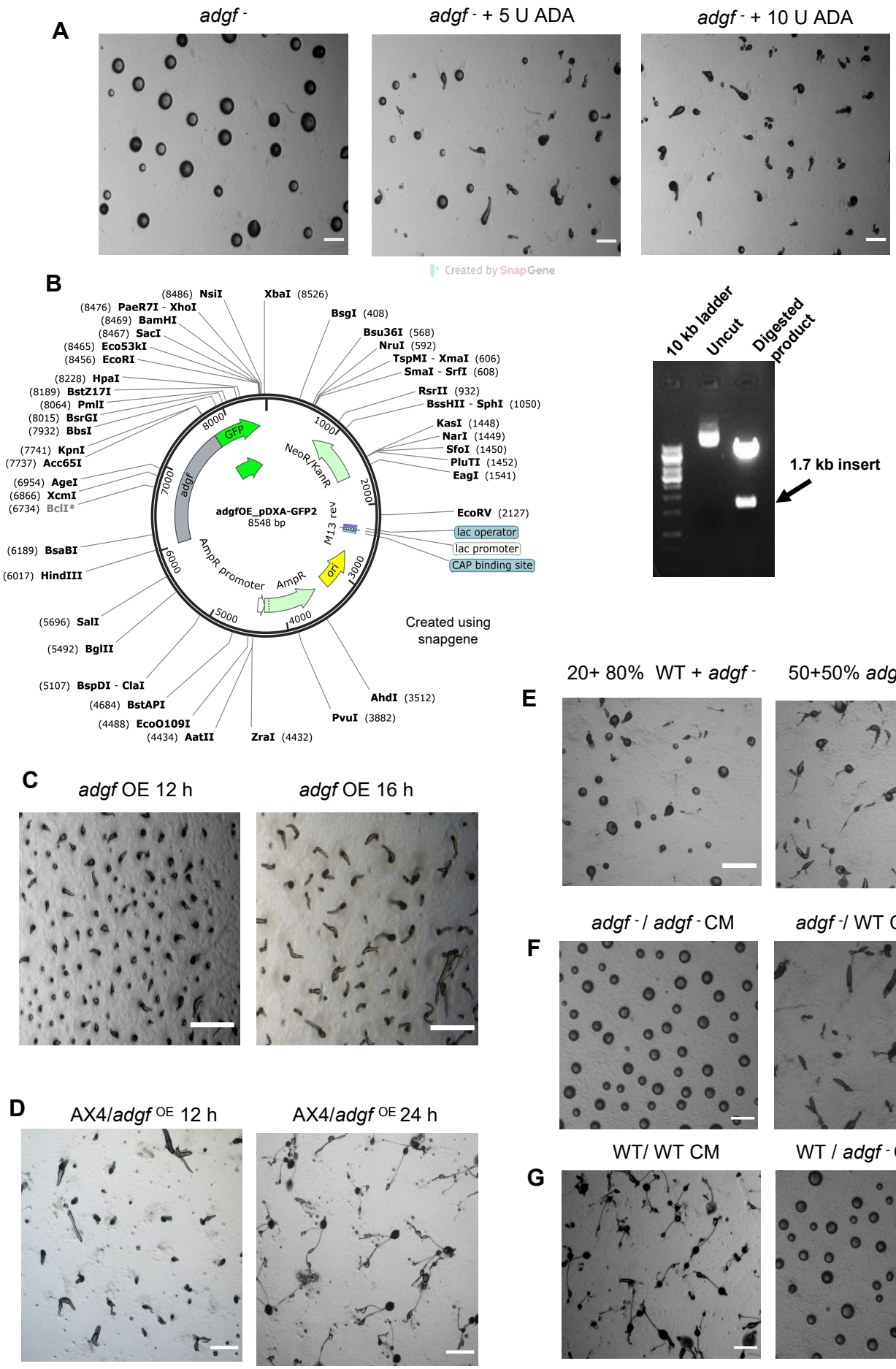
A
adgf -
adgf - + 5 U ADA
adgf - + 10 U ADA
B
Created by SnapGene
(8486) NsiI
XbaI (8526)
(8476) PaeR7I - XhoI
(8469) BamHI
(8467) SacI
(8465) Eco53kI
(8456) EcoRI
(8228) HpaI
(8189) BstZ17I
(8064) PmlI
(8015) BsrGI
(7932) BbsI
(7741) KpnI
(7737) Acc65I
(6954) AgeI
(6866) XcmI
(6734) BclI*
(6189) BsaBI
(6017) HindIII
(5696) SalI
(5492) BglII
(5107) BspDI - ClaI
(4684) BstAPI
(4488) EcoO109I
(4434) AatII
ZraI (4432)
PvuI (3882)
AhdI (3512)
BsgI (408)
Bsu36I (568)
NruI (592)
TspMI - XmaI (606)
SmaI - SrfI (608)
RsrII (932)
BssHII - SphI (1050)
KasI (1448)
NarI (1449)
SfoI (1450)
PluTI (1452)
EagI (1541)
EcoRV (2127)
lac operator
lac promoter
CAP binding site
1000
2000
3000
4000
5000
6000
7000
8000
GFP
adgf
NeoR/KanR
M13 rev
ori
AmpR
AmpR promoter
adgfOE_pDXA-GFP2
8548 bp
Created using
snapgene
10 kb ladder
Uncut
Digested
product
1.7 kb insert
C
adgf OE 12 h
adgf OE 16 h
D
AX4/adgf OE 12 h
AX4/adgf OE 24 h
E
20+ 80% WT + adgf -
50+50% adgf - + WT
F
adgf - / adgf - CM
adgf -/ WT CM
G
WT/ WT CM
WT / adgf - CM

Figure 4. Overexpression of *adgf* rescued the mound arrest phenotype

A) *adgf*$^-$ mounds were treated with 5 U and 10 U ADA enzyme, and imaged at 16 h. Scale bar: 2 mm; (n=3). **B)** The full-length *adgf* gene was cloned in the vector pDXA-GFP2. The overexpression construct was verified by restriction digestion with HindIII and KpnI enzymes. **C)** *adgf* overexpression in the mutant rescued the mound arrest. **D)** Overexpression of *adgf* in WT background. Scale bar: 2 mm; (n=3). The time points in hours are shown at the top. **WT cells mixed with *adgf*$^-$ rescued the *adgf* mutant phenotype. E)** Mixing of WT with *adgf*$^-$ in a 1:4 ratio showed a partial rescue, and a full rescue of the *adgf*$^-$ mound arrest phenotype in a 1:1 ratio with WT. **F)** Development of *adgf* mutants in the presence of *adgf*$^-$ CM and WT CM on KK2 agar plates. WT CM rescued the mound arrest. **G)** Development of WT in the presence of WT CM and *adgf*$^-$ CM on KK2 agar plates. *adgf*$^-$ CM induced mound arrest in WT cells. Scale bar: 2 mm; (n=3).

Figure 5

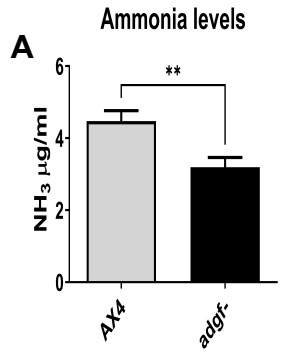
A
Ammonia levels
**
NH3 µg/ml
0
2
4
6
AX4
adgf-

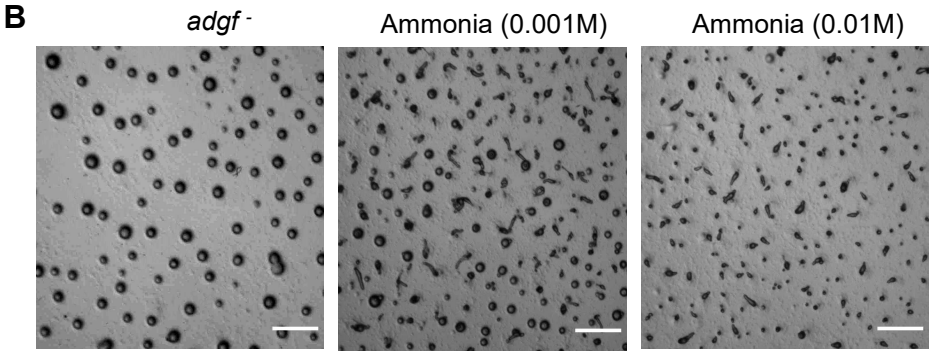
B
adgf -
Ammonia (0.001M)
Ammonia (0.01M)

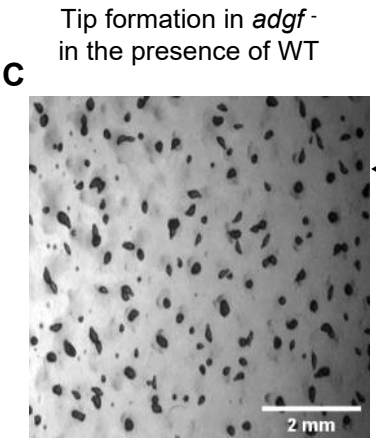
C
Tip formation in adgf -
in the presence of WT
2 mm

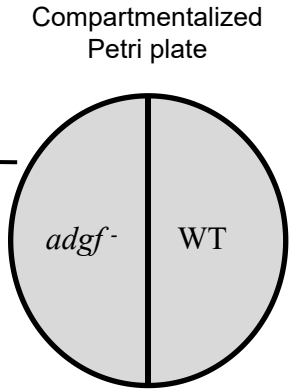
Compartmentalized
Petri plate
adgf -
WT

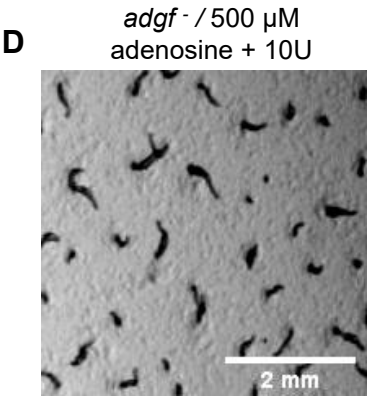
D
adgf - / 500 µM
adenosine + 10U
2 mm

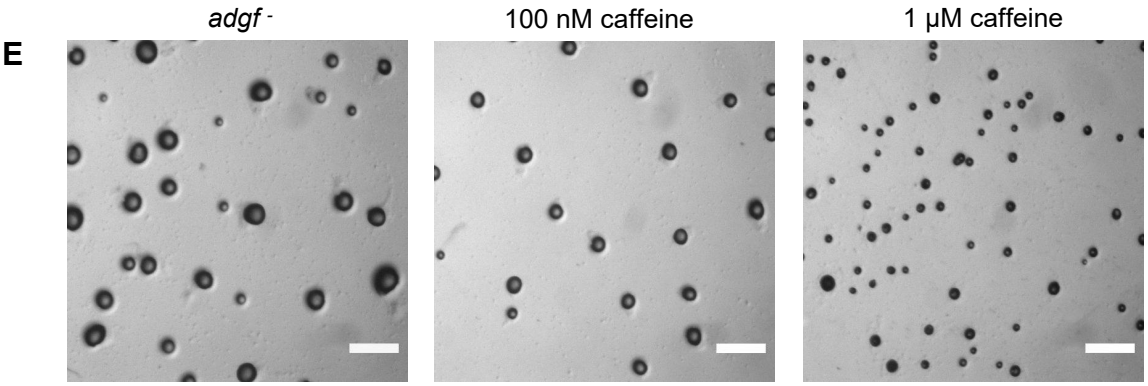
E
adgf -
100 nM caffeine
1 µM caffeine

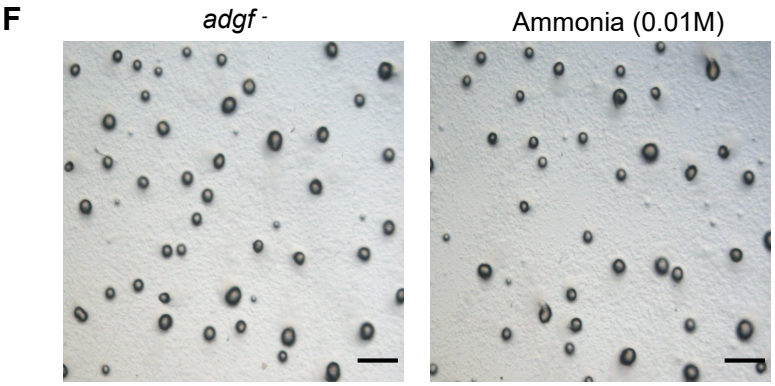
F
adgf -
Ammonia (0.01M)

Figure 5. Adenosine deamination reaction rescues the mound arrest of *adgf* $^{-}$

A) Quantification of ammonia using the ammonia assay kit. WT and *adgf* $^{-}$ mounds were harvested and lysed using a cell lysis buffer. Cell debris was removed by centrifugation, and the supernatant was used to quantify ammonia. **B)** Treatment of *adgf* $^{-}$ mounds with ammonia. Ammonia was generated by mixing 2 ml of NH_4Cl and 2 ml of 1N NaOH. The mixture was poured on top of the lid and the KK2 plates with the mounds were inverted and sealed thereafter. Images were taken 3.5 h post treatment. Dose dependent effect of ammonia on the rescue. Scale bar: 2 mm; (n=3). **C)** WT and *adgf* $^{-}$ cells on either side of a compartmentalized Petri dish led to tip fornation in *adgf* $^{-}$. **D)** *adgf* $^{-}$ cells on one side and KK2 buffer containing adenosine and ADA on the other side of the compartmentalized dish, rescued the mound defect. **Caffeine rescues the large mound size of *adgf* mutant. E)** *adgf* $^{-}$ cells were treated with different concentrations of caffeine (100 nM, 1 µM) while plating, and images were taken during mound stage. Scale bar: 2 mm; n=3. **F)** Exposure to ammonia does not rescue the mound size of *adgf* mutant. *adgf* $^{-}$ mounds were exposed to 0.01 M ammonia and images were captured 3.5 h post chemical treatment. Scale bar: 2 mm; (n=3).

Figure 6

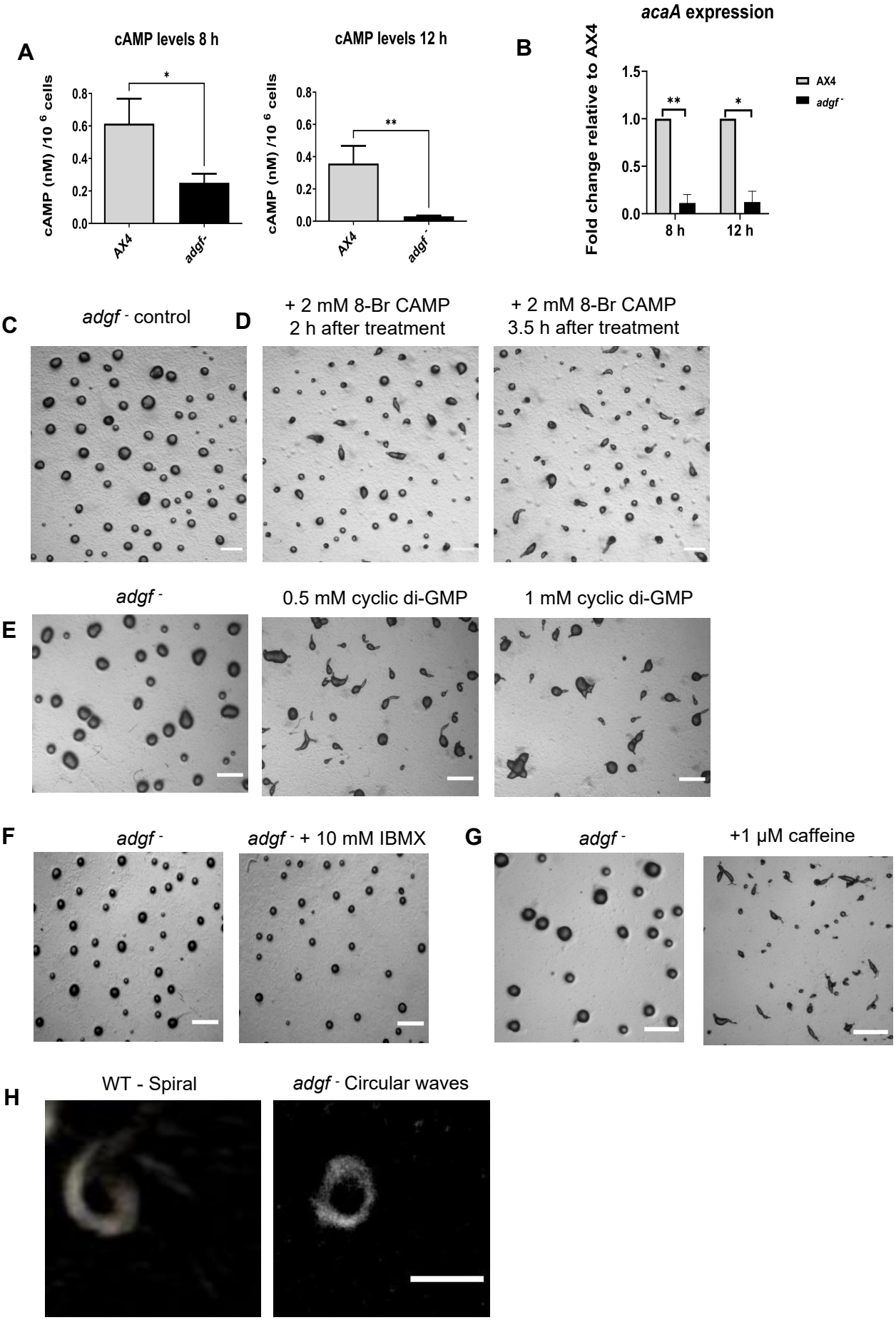
A
cAMP levels 8 h
cAMP levels 12 h
cAMP (nM) /10 6 cells
0.0
0.2
0.4
0.6
0.8
*
**
AX4
adgf-
B
acaA expression
Fold change relative to AX4
0.0
0.5
1.0
1.5
**
*
8 h
12 h
AX4
adgf -
C
adgf - control
D
+ 2 mM 8-Br CAMP
2 h after treatment
+ 2 mM 8-Br CAMP
3.5 h after treatment
E
adgf -
0.5 mM cyclic di-GMP
1 mM cyclic di-GMP
F
adgf -
adgf - + 10 mM IBMX
G
adgf -
+1 μM caffeine
H
WT - Spiral
adgf - Circular waves

Figure 6. Impaired cAMP signaling in *adgf*$^{-}$

A) Total cAMP levels in WT and *adgf*$^{-}$ mounds were quantified using cAMP-XP assay kit (Cell signaling, USA). Level of significance is indicated as *$p < 0.05$, **$p < 0.01$; (n=3). **B)** *acaA* expression was quantified using qRT-PCR. The error bars represent the mean ± SEM (n=3). **C)** *adgf*$^{-}$ mounds. **D)** Time course of *adgf*$^{-}$ mounds treated with 8-Br-cAMP and imaged at different intervals. Scale bar: 2 mm; (n=3). **Treatment with cyclic di-GMP and caffeine rescues the mound arrest phenotype. E)** Addition of cyclic-di-GMP restored tip formation in *adgf*$^{-}$ 3.5 h after the treatment. Scale bar: 1 mm; (n=3). **F)** PDE inhibitor (IBMX) treatment failed to rescue the *adgf*$^{-}$ mound arrest. Scale bar 1 mm; (n=3). **G)** *adgf*$^{-}$ mounds treated with caffeine formed tips 3.5 h post treatment. Scale bar: 2 mm; (n=3). **Altered cAMP wave pattern in *adgf* mutants. H)** Optical density waves depicting cAMP wave generating centers in WT and *adgf*$^{-}$. WT shows spiral and *adgf*$^{-}$ exhibits circular wave propagation.

Figure 7

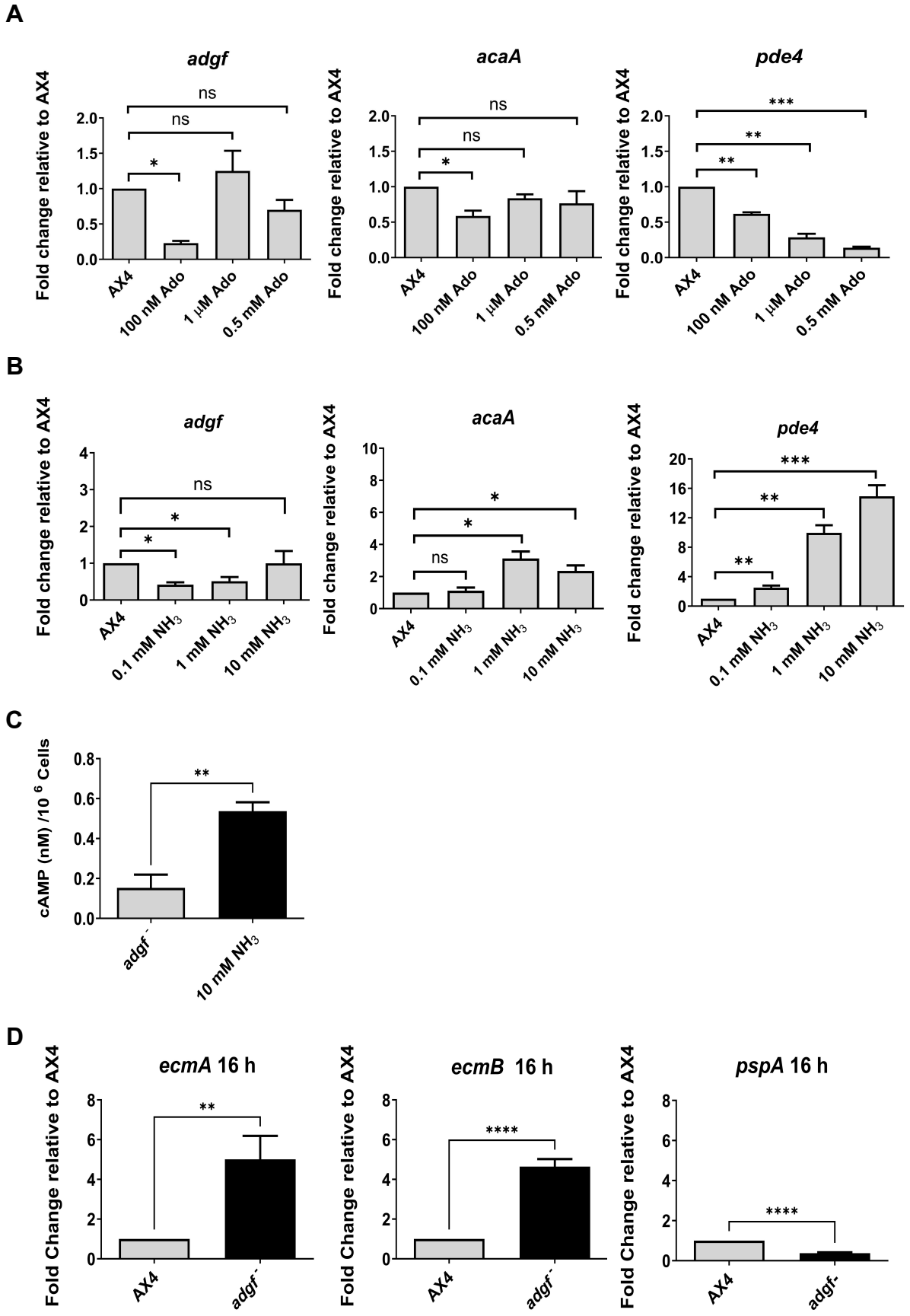
A
adgf
acaA
pde4
Fold change relative to AX4
ns
*
**
***
AX4
100 nM Ado
1 μM Ado
0.5 mM Ado
B
0.1 mM NH3
1 mM NH3
10 mM NH3
C
cAMP (nM) /10 6 Cells
adgf-
D
ecmA 16 h
ecmB 16 h
pspA 16 h
****

Figure 7. Expression levels of *adgf*, *acaA* and *pde4* in response to adenosine and ammonia treatment

A) Expression levels of *adgf*, *acaA* and *pde4* in response to adenosine treatment (100 nM, 500 nM, 1 µM). **B)** And ammonia treatment (0.1 mM, 1 mM, 10 mM). Level of significance is indicated as *p<0.05, **p<0.01, and ***p<0.001; (n=3). **C)** cAMP levels in *adgf* mutants rescued with ammonia. Level of significance is indicated as **p< 0.01; (n=3). **Expression levels of prestalk (pst), *ecmA, ecmB* and prespore (psp), *pspA* cell type markers in *adgf*$^-$.** The expression profile of **D)** pst (*ecmA*, *ecmB*) and psp (*pspA*) specific markers in WT and *adgf*$^-$ were quantified using qRT-PCR. Level of significance is indicated as **p<0.01 and ****p<0.0001; (n=3). Three independent biological replicates were performed and the error bars represent the mean and SEM. The fold-change in RNA transcript levels is relative to WT at the indicated time points. *rnlA* was used as the internal control (n=3). ns = not significant.

Figure 8

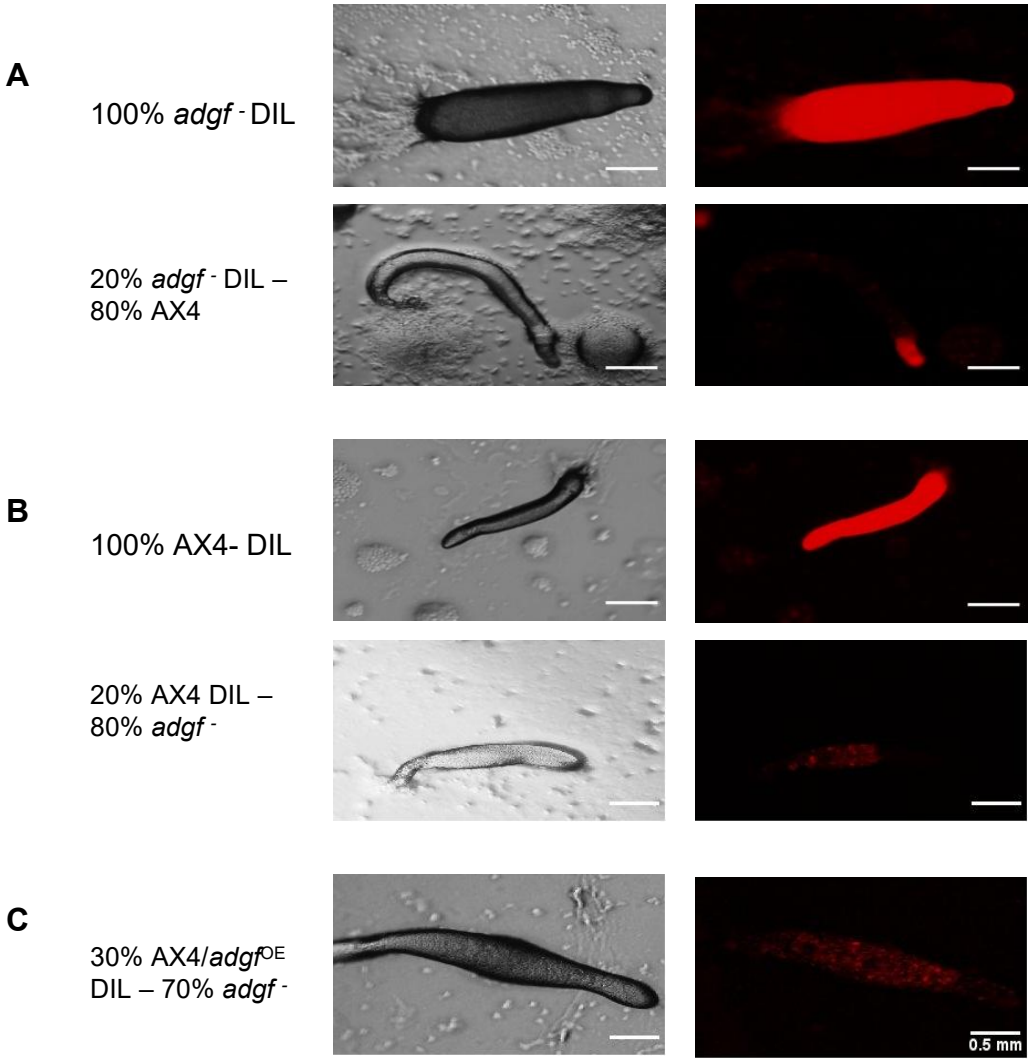

Figure 8. Mixing of WT cells with *adgf* - following DIL staining

A-C) DIL labelled cells were mixed with unlabelled cells and plated on KK2 agar. Images were captured during the migrating slug stage. The left panel shows bright field, and the right panel shows the corresponding fluorescence images. Scale bar: 0.5 mm; (n=3).

Figure 9

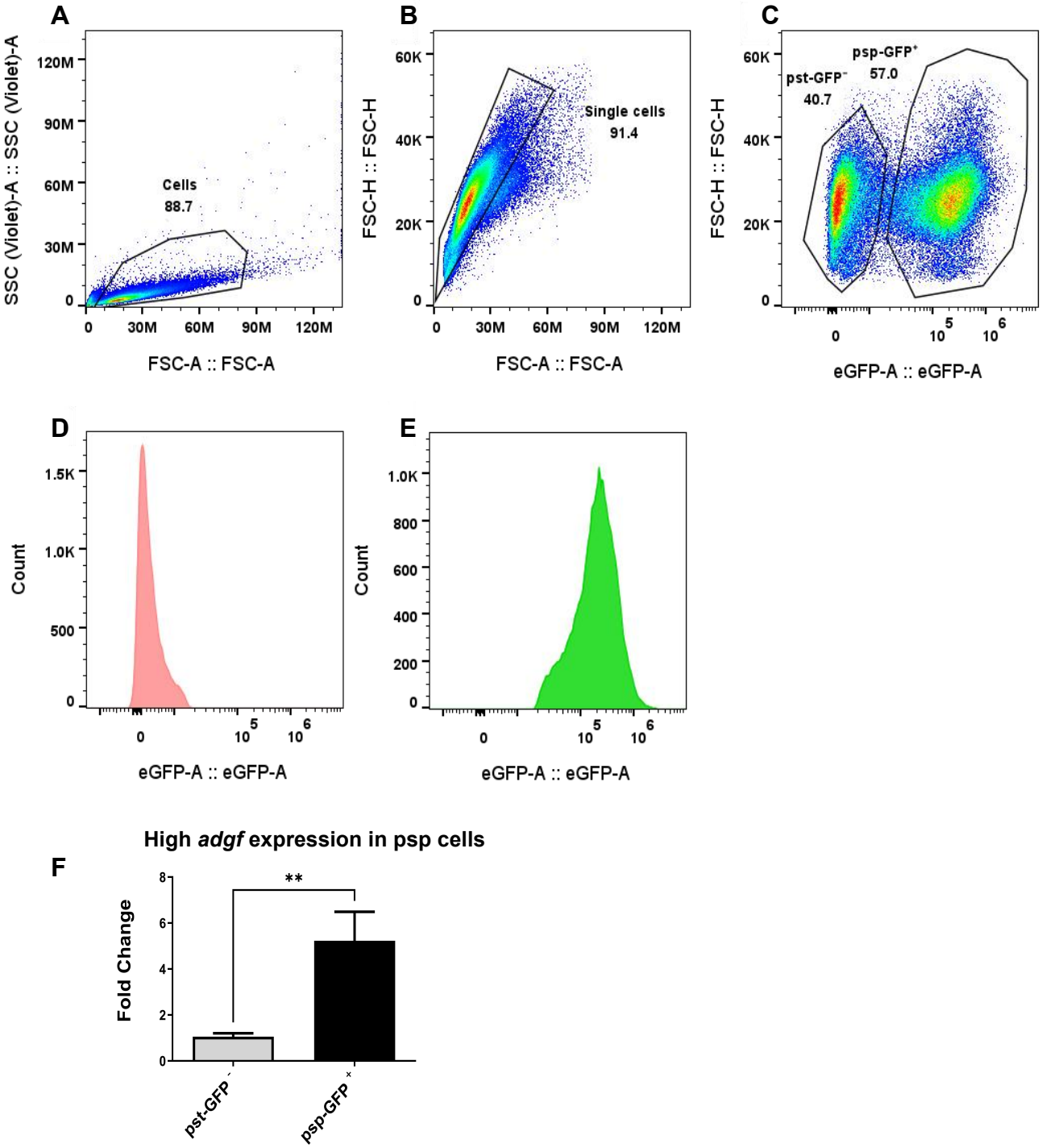

Figure 9. Sorting of pst-GFP⁻ and psp-GFP⁺ *Dictyostelium* cells by fluorescence activated cell sorter

A) Forward scatter (FSC) vs. side scatter (SSC) plot used to gate total cells. **B)** Singlets were gated based on FSC-H vs. FSC-A to exclude doublets and aggregates. **C)** GFP fluorescence profile of gated single cells reveals two populations: pst-GFP⁻ and psp-GFP⁺, corresponding to pst and psp cells, respectively. **D)** GFP⁻ (pst) and **E)** GFP⁺ (psp) fractions. **F)** *adgf* expression in FACS sorted samples was quantified by qRT-PCR. Level of significance is indicated as **$p<0.01$ (n=3).

Figure 10

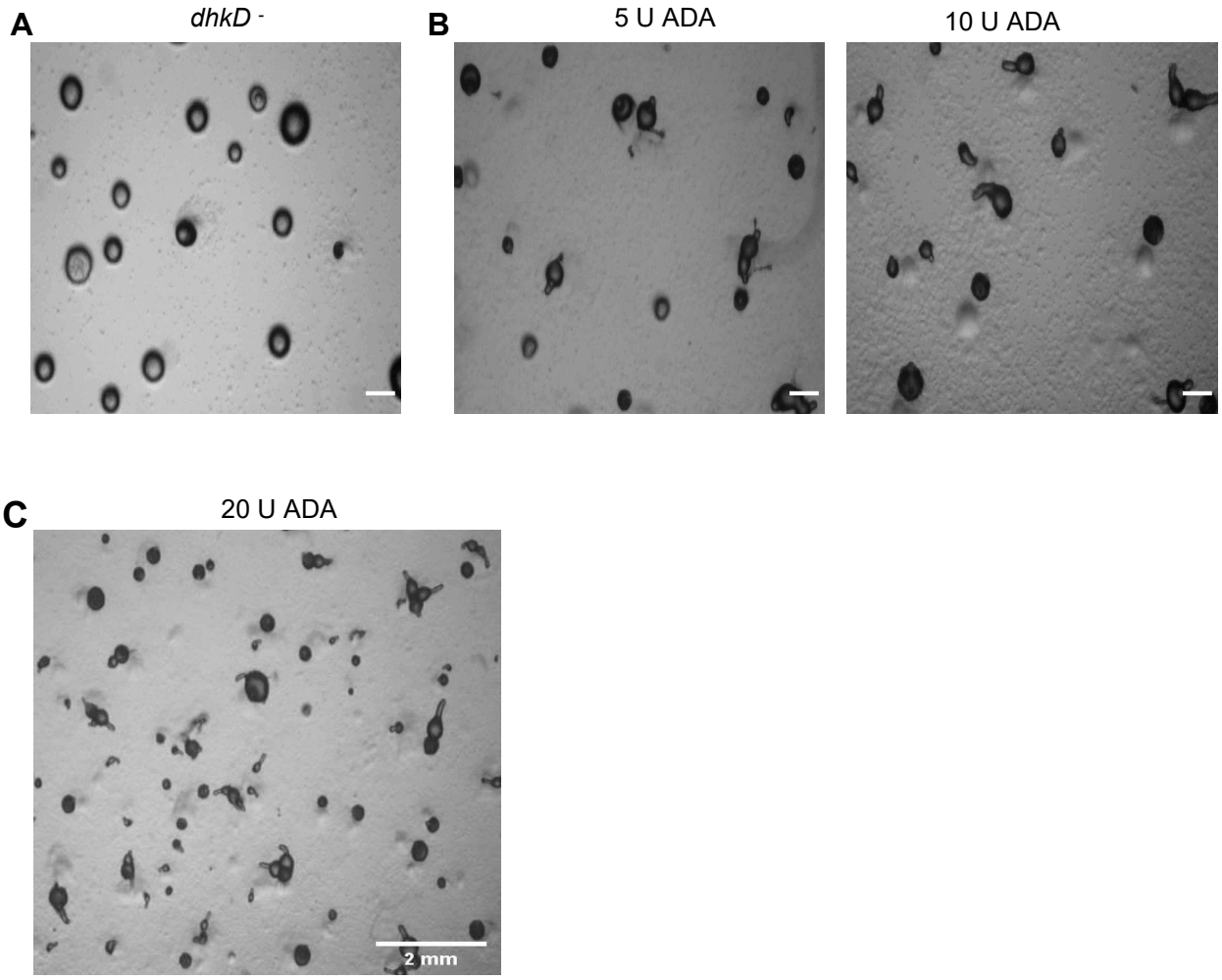

Figure 10. *adgf* acts downstream of the histidine kinase *dhkD*

A) *dhkD* mutants on KK2 agar plates. **B)** 5 U, 10 U ADA rescued the mound arrest phenotype in a dose dependent manner. Scale bar: 1 mm; (n=3). Images were taken 3.5 h post treatment. **C)** Addition of 20 U ADA led to formation of multiple tips. Scale bar: 2 mm; (n=3).

Figure 11

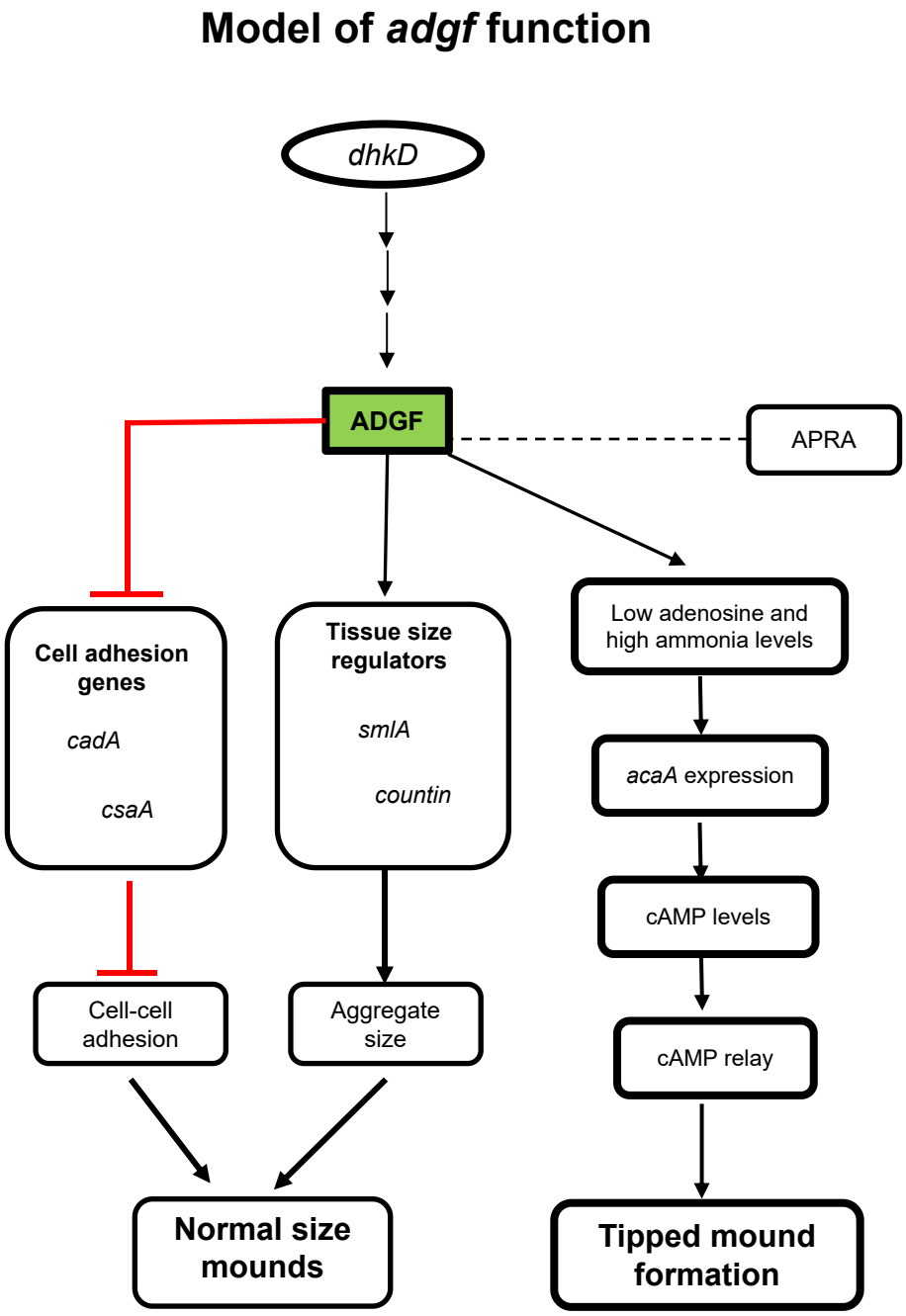

Figure 11. Model illustrating the role of *adgf* in development

adgf suppresses the expression of genes involved in cell adhesion, *cadA* and *csaA,* and regulates the mound size and tip development by directly acting on adenosine, ammonia levels and cAMP signaling. Line ending in an arrow indicates that the previous gene/factor either directly or indirectly raises the activity or levels of the second; line ending in a cross-bar indicates inhibition. Dotted lines indicate ADGF interacting with APRA.